

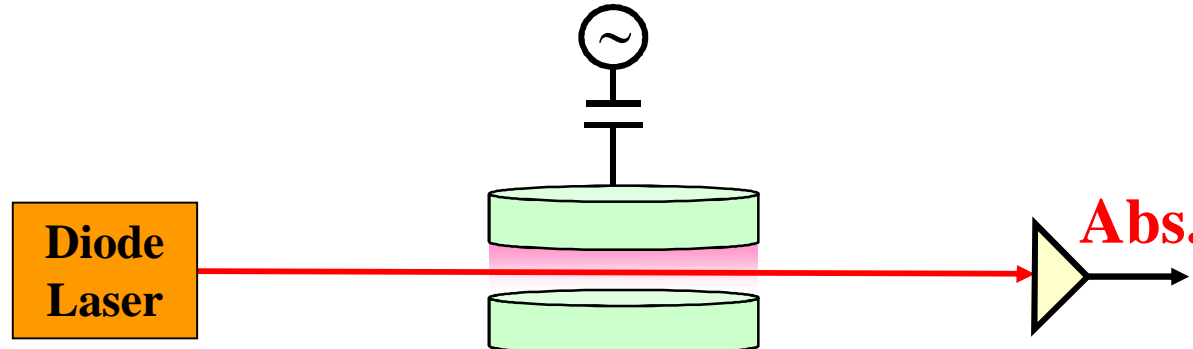
Diagnostics des plasmas par absorption optique; de Mitchell et Zemansky à la CRDS

Nader SADEGHI

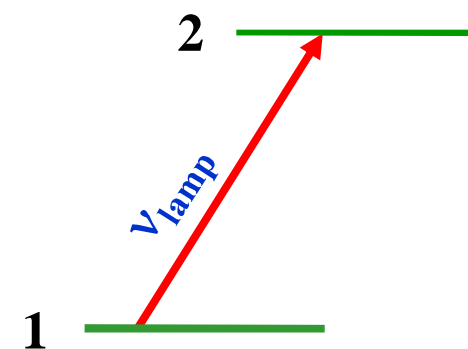
*Laboratoire Interdisciplinaire de Physique (LIPhy) &
Laboratoire des Technologies de la Microelectronique (LTM),
Université de Grenoble & CNRS Grenoble, France
E-mail: Nader.Sadeghi@ujf-grenoble.fr*



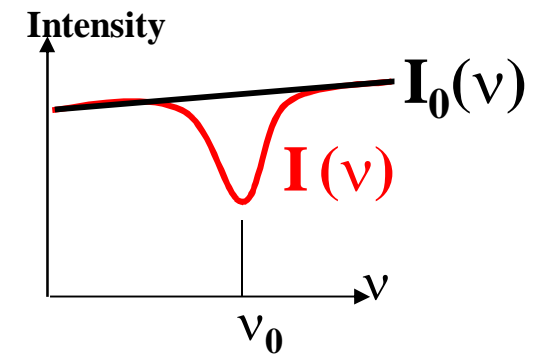
Optical Absorption Spectroscopy (Laser Absorption):



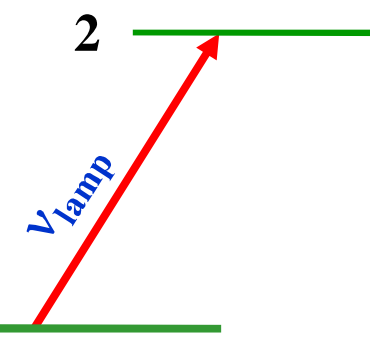
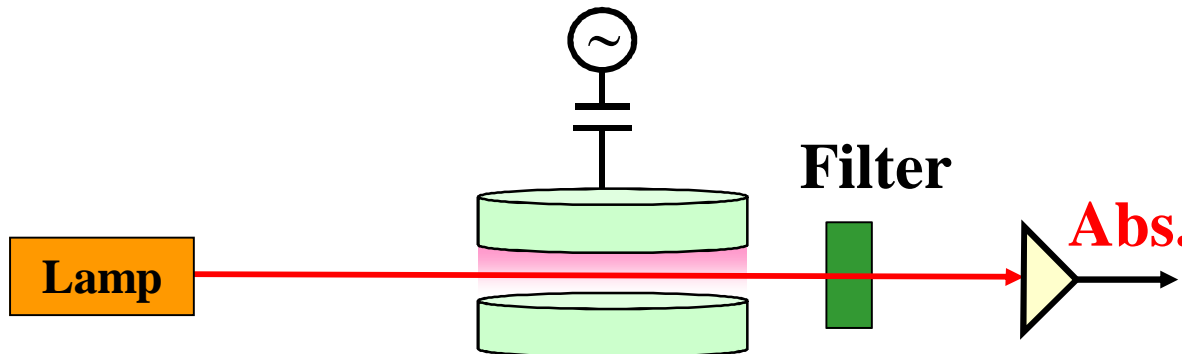
1- Light source is a tunable laser



$$\int L n \left(\frac{I_0(\nu)}{I(\nu)} \right) d\nu \propto < N.l >.B$$

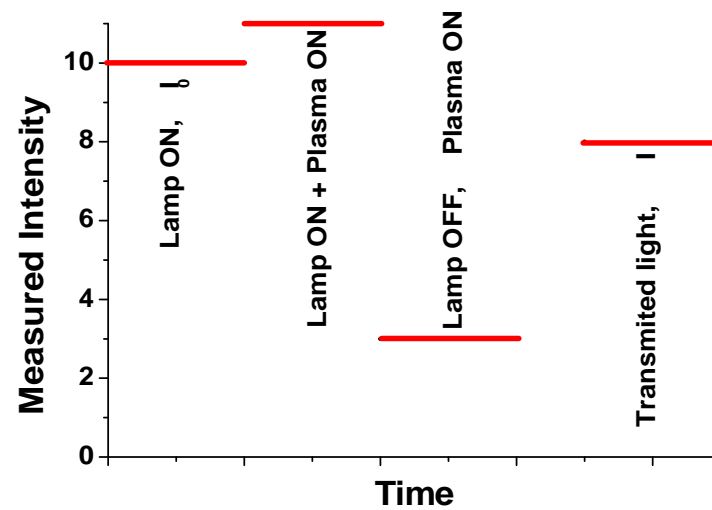


Resonance Absorption

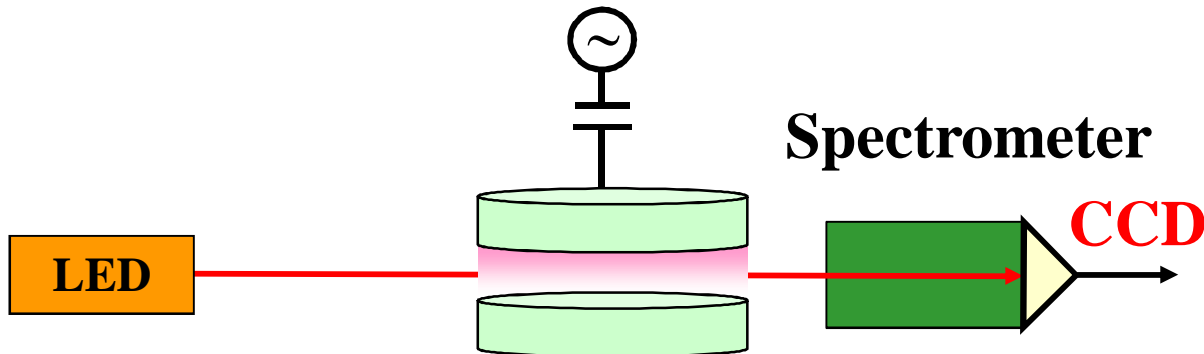


2- Light source emits the absorption line

- A hollow cathode lamp for the detection of metal atoms

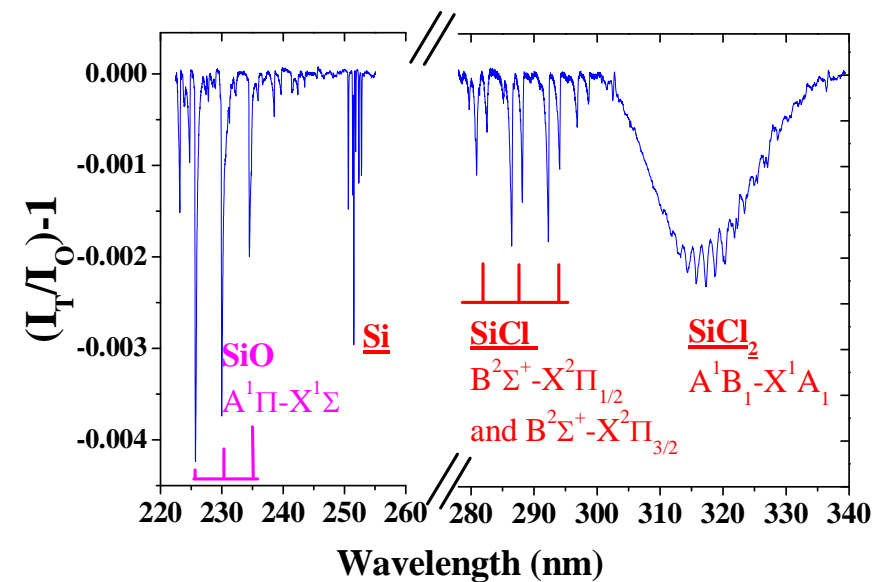
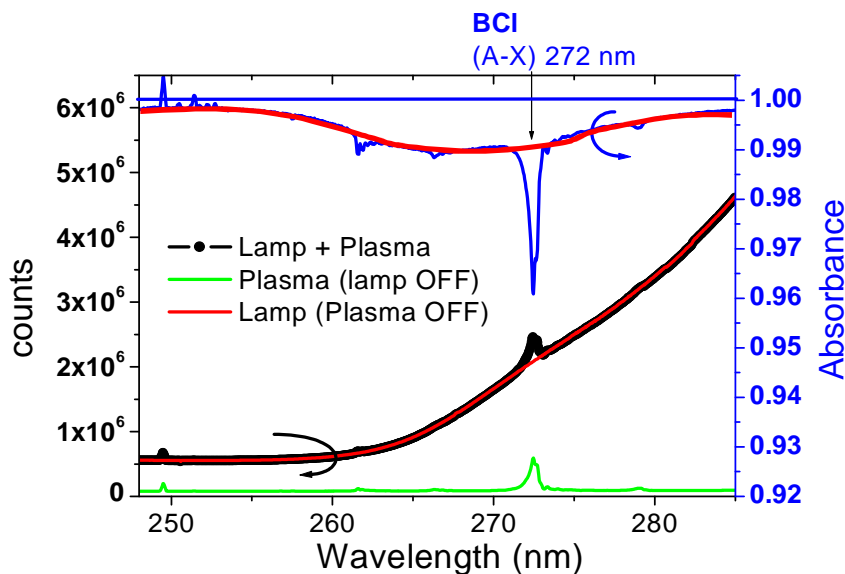


Broad-Band Absorption

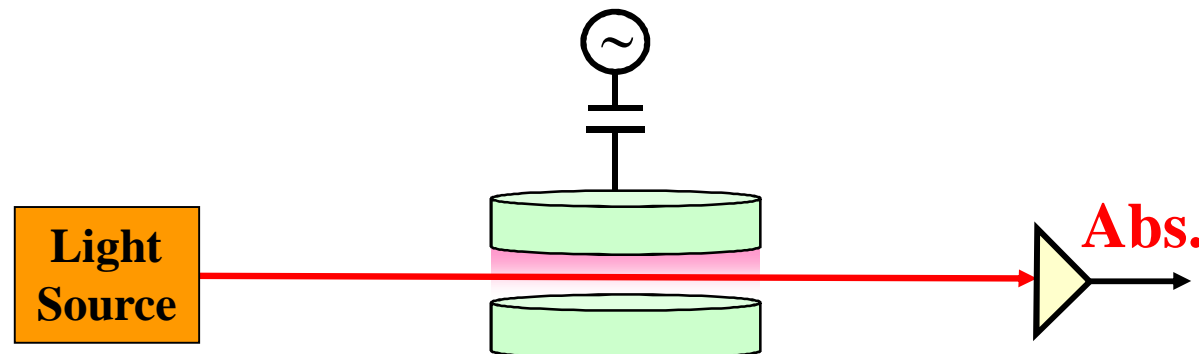


3- Broad-Band Light source

- An Arc lamp, LED or a femtosecond laser

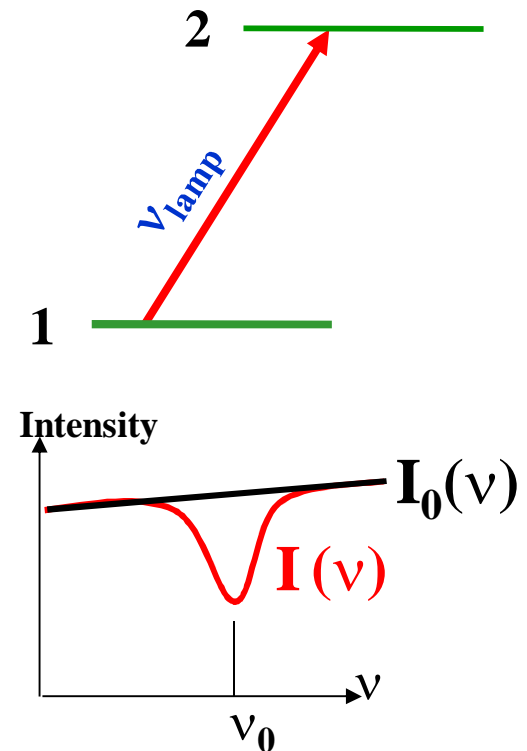


Advantages and drawback of OAS



-It provides the absolute density of absorbing species:

$$\int \ln\left(\frac{I_0(\nu)}{I(\nu)}\right) d\nu \propto < N.l >.B$$



- But this will be a line of sight averaged value

Outline

É Resonance absorption Spectroscopy

- ó Main artifact: line profile
- ó Self Absorption

É Broad Band absorption

- ó Use of LED as light source
- ó VUV application
- ó Main artifact: Spectral resolution

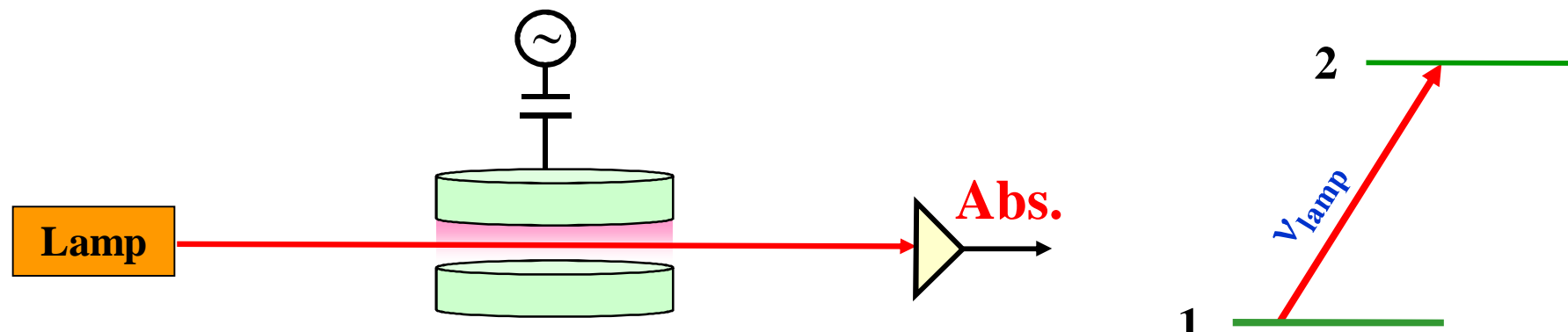
É Tunable laser absorption techniques:

- ó A few applications of Single pass absorption
- ó Main artifact: Optical saturation phenomena

É High sensitivity techniques (Cavity enhanced)

Resonance absorption technique

Principle of Resonance Absorption on a single line



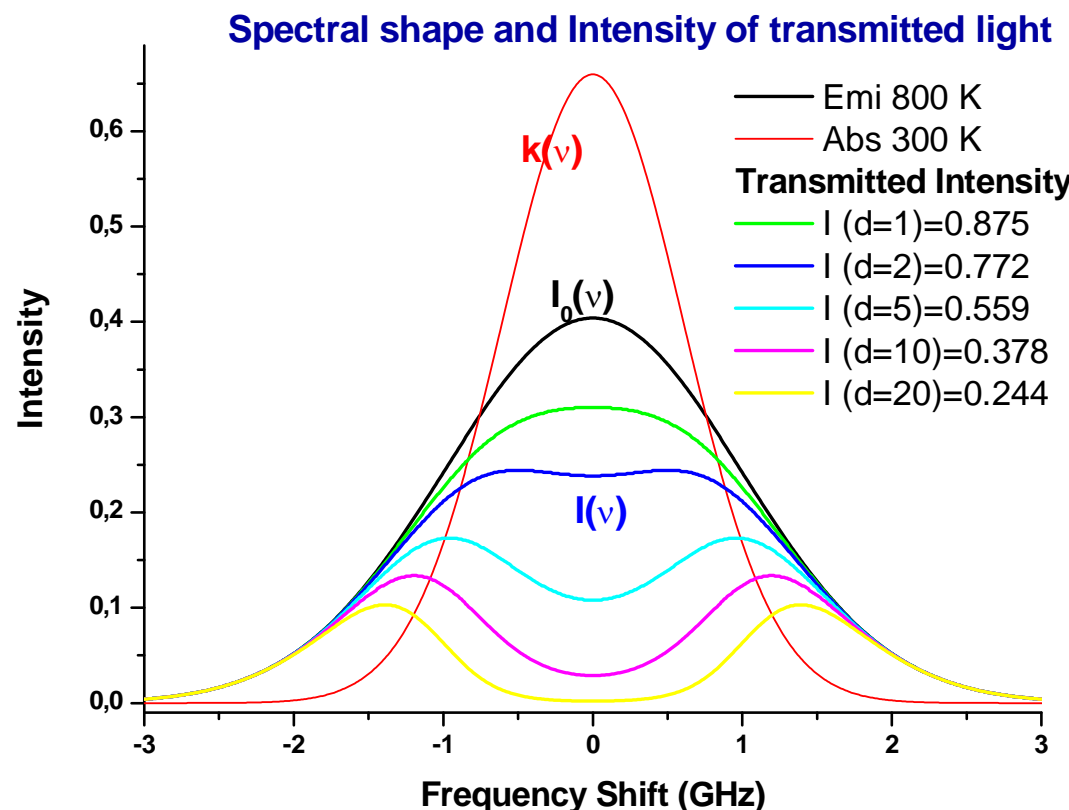
- A lamp which emits transitions of the same element serves as light source
- This is usually another plasma: Hollow cathode lamp for the detection of metal atoms

A low current (≈ 10 mA) discharge in neon sputters metal atoms from a $\phi_i=3$ mm, $l=15$ mm hollow cylinder and excites them

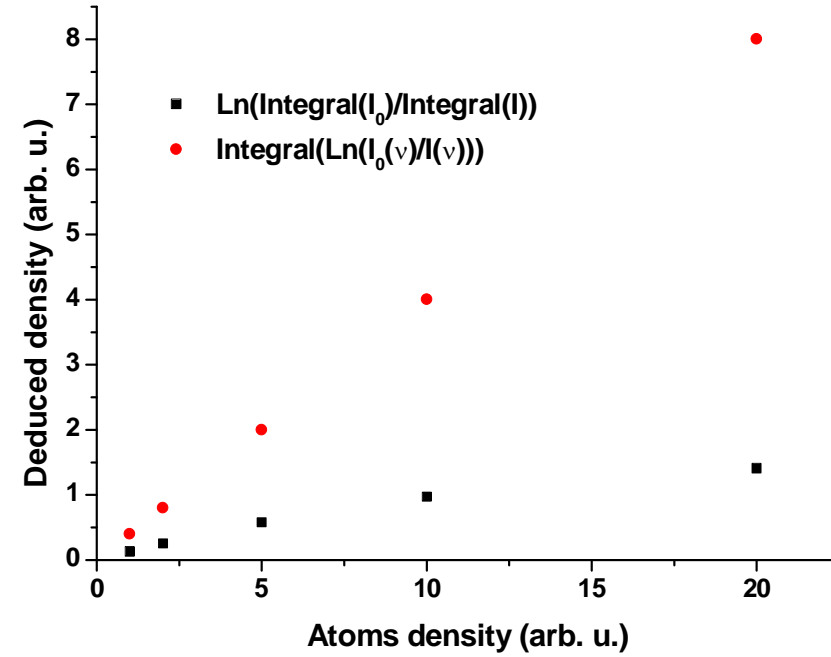
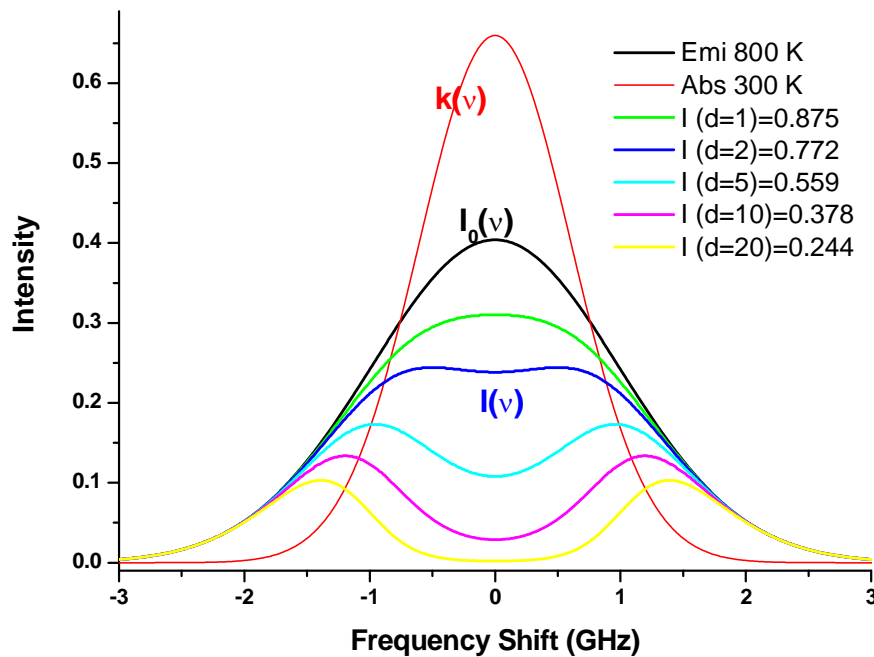


Principle of Resonance Absorption on a single line

Assuming Gaussian profiles for both Emission of the lamp and absorption in the plasma, the spectral profiles of the transmitted light at different absorbing atoms density are:



Principle of Resonance Absorption on a single line



$\ln \left[\int I_0(\lambda) d\lambda / \int I(\lambda) d\lambda \right]$ would provide a wrong results

the correct result could be obtained if it was possible to calculate

$$\int \ln[I_0(\lambda) / I(\lambda)] d\lambda$$

Resonance absorption for density measurement

- Lamp emission spectral profile: $I(\lambda) = I_0 \cdot \frac{2 \cdot \sqrt{\ln(2)}}{\Delta\lambda_{De} \cdot \sqrt{\pi}} \text{Exp}(-4 \cdot \ln(2) \cdot (\lambda - \lambda_0)^2 / \Delta\lambda_{De}^2)$

- Absorption spectral profile: $k(\lambda) = k_0 \cdot \frac{2 \cdot \sqrt{\ln(2)}}{\Delta\lambda_{Da} \cdot \sqrt{\pi}} \text{Exp}(-4 \cdot \ln(2) \cdot (\lambda - \lambda_0)^2 / \Delta\lambda_{Da}^2)$

- *Doppler width:* $\Delta\lambda_D = 7.16 \times 10^{-7} \lambda_0 (T/M)^{1/2}$ and $k_0 \propto f \cdot [N_a]$

- Intensity of the transmitted light: $I^T = \int I(\lambda) \cdot \text{Exp}(-L \cdot k(\lambda)) d\lambda$

From Mitchell and Zemansky:

- Absorption rate: $A_L = 1 - \frac{I^T}{I_0} = \sum_{m=1}^{\infty} \frac{(-1)^{m+1}}{m!} \frac{(k_0 L)^m}{\sqrt{1 + m \cdot \alpha^2}}$ where $\alpha^2 = T_e/T_a$

When the oscillator strength f , the absorption length L , and α are known, the absorbing atoms density $[N_a]$ can be deduced from A_L measurement.

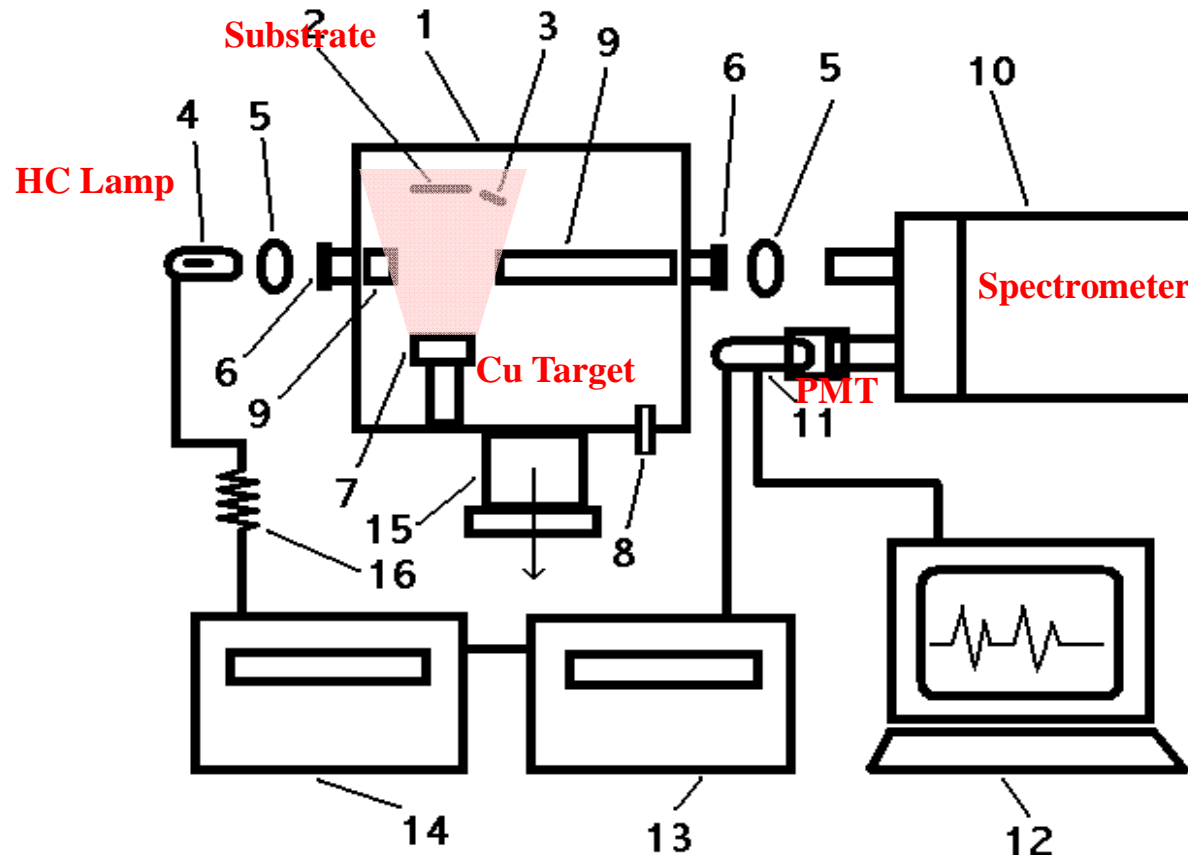
But the above relation holds only for a single line with Doppler profiles

Measuring copper atoms density in magnetron discharge

Work published: H. Naghshara *et al*, J. Phys. D: Appl. Phys. **44 (2011) 025202**

Experimental set-up

Magnetron discharge with Cu target



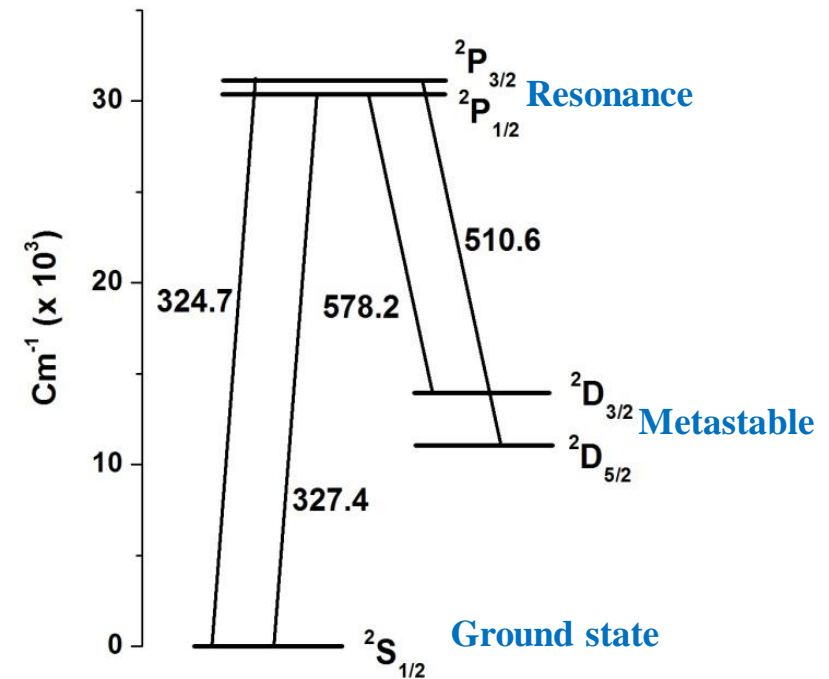
dc magnetron discharge:

- Chamber $\phi_i=60$ cm, h=50 cm
- 0.3 - 14 μ bar argon pressure
- 10 - 200 W of dc power

Cu energy levels of interest

Resonance absorption with a Copper Hollow Cathode Lamp

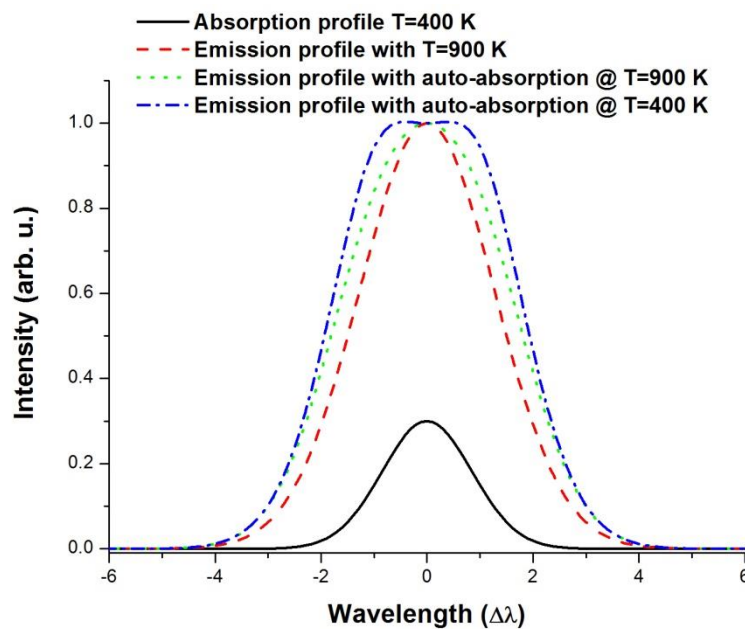
- Density of Cu($^2S_{1/2}$) with 327.4 nm line
- Density of Cu($^2D_{5/2}$) with 510.6 nm line
- Cu deposition rate with a microbalance
- Gas temperature from N₂, 337 nm band with a few% nitrogen added as tracer



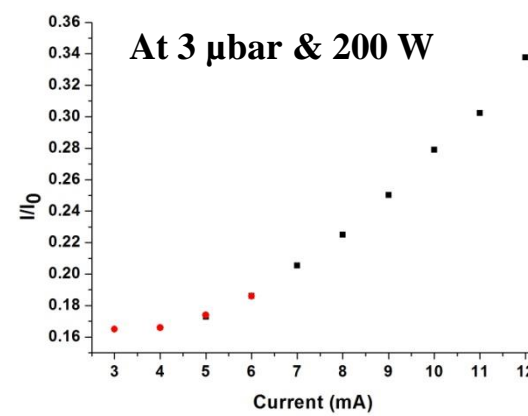
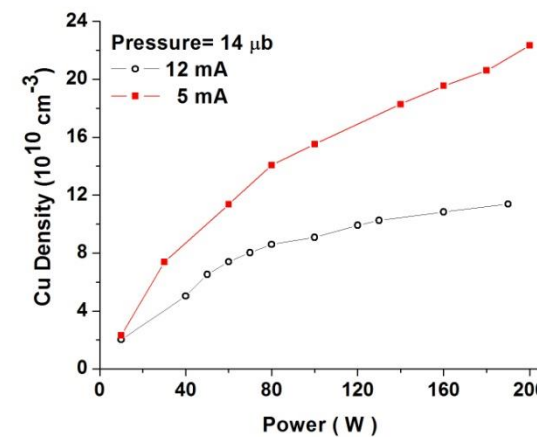
Influence of auto-absorption inside the HC Lamp on absorption measurements

Absorption of photons emitted on copper resonance lines from the deepest part of the HCL by Cu atoms of the outer part of the HCL can modify the emission line profile, which becomes non Gaussian.

Higher is the Cu density, stronger is the perturbation.

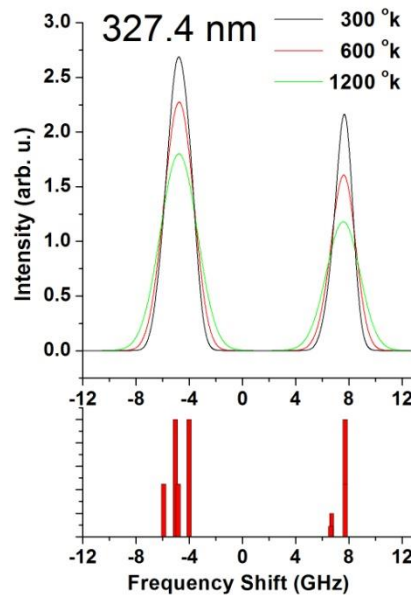


$$I/I_0 = \Phi(\text{absorbing atoms density})$$

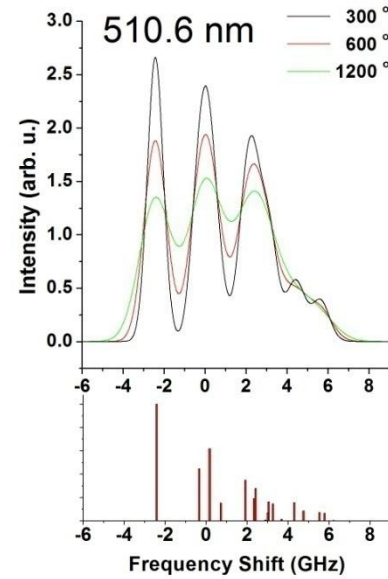


Influence of line structure

Copper has two isotopes: ^{63}Cu (69%) and ^{65}Cu (31%), both with $I=3/2$ nuclear spin. Due to the isotopic shift and hyperfine structure of energy levels, all copper lines are no more single but have many components.



Frequency shifts and relative intensities of the 8 components of the 327.4 nm line (bottom) and the spectral profile of the line at different temperatures (top).



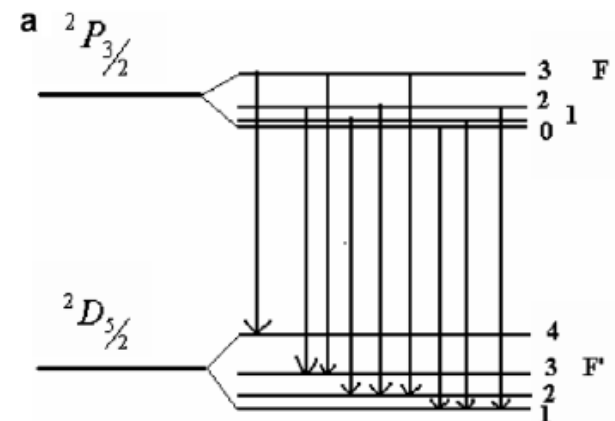
Frequency shifts and relative intensities of the 18 components of the 510.6 nm line (bottom) and the spectral profile of the line at different temperatures (top).

Hyperfine splitting and isotope shift of energy levels

$$\Delta v = \frac{AC}{2} + \frac{B}{4} \frac{3/2C(C+1) - 2I(I+1)J(J+1)}{IJ(2I-1)(2J-1)}$$

$$C = F(F+1) - J(J+1) - I(I+1) \quad |J-I| \leq F \leq |J+I|$$

J= Total angular momentum; I= nuclear Spin



Isotope	Level	A (MHz)	B (MHz)	Isotope shift relative to ^{63}Cu (MHz)
^{63}Cu	$^2S_{1/2}$	5866.9 (a)	-	
	$^2P_{1/2}$	506.9 (b)	-	
	$^2P_{3/2}$	195.2 (c)	-28.8 (c)	
	$^2D_{5/2}$	749.1 (b)	186.0 (b)	
^{65}Cu	$^2S_{1/2}$	6284.4 (a)	-	<u>540</u> (d)
	$^2P_{1/2}$	543.3 (b)	-	0 (e)
	$^2P_{3/2}$	209.1 (c)	-26.6 (c)	-30 (e)
	$^2D_{5/2}$	803.6 (b)	174.3 (b)	-2280 (e)

Spectroscopic constants A (magnetic dipole), B (electric quadrupole) and isotope shift of different states of Cu considered in this work.

Frequency shifts and relative intensities of different components of the lines

		63 Cu		65 Cu		
$F\ddot{o}$	$F\phi$	$\hat{\epsilon}$ (MHz)	I	$\hat{\epsilon}$ (MHz)	I	
1	0	3034	16.7	5529	7.5	510.6 nm
1	1	3258	15	5765	6.7	
1	2	3677	1.7	6210	0.8	
2	1	1909	35	4297	15.7	
2	2	2328	19.4	4742	8.7	
2	3	2885	1.1	5343	0.5	
3	2	164	62.2	2409	28	
3	3	721	15.6	3011	7	
4	3	-2423	100	-343	45	
1	1	6700	20	6636	9	327.4 nm
1	2	7713	100	7723	45	
2	1	-5033	100	-5932	45	
2	2	-4020	100	-4845	45	
1	0	6565	14.3	6468	6.4	324.7 nm
1	1	6789	35.7	6703	16	
1	2	7208	35.7	7148	16	
2	1	-4945	7.1	-5865	3.1	
2	2	-4525	35.7	-5421	16	
2	3	-3969	100	-4820	44.9	

Frequency shift (MHz) and relative intensity (deduced from quantum mechanics calculations) of different components of 510.6, 327.4 and 324.7 nm lines in both emission and absorption. For each line, the intensity of the strongest component is normalized to 100.

Influence of the line structure

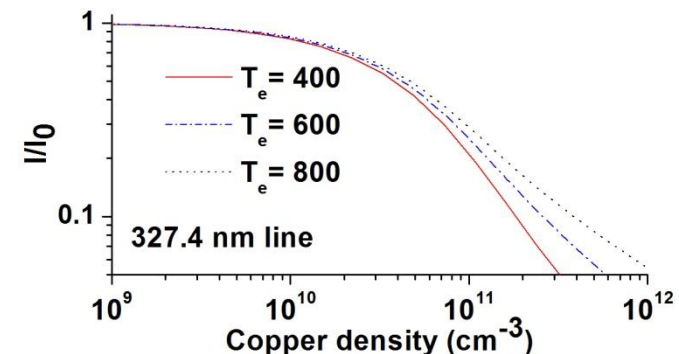
The correct equations for the line intensity and absorption coefficients are:

$$I(\lambda) = I_0 \frac{2}{\Delta\lambda_{De}} \sqrt{\frac{\ln 2}{\pi}} \frac{1}{\sum_k (\rho_k \sum_{F'F''} S_{F'F''})} \times \sum_k \rho_k \sum_{F'F''} S_{F'F''} \text{Exp} \left[-4(\ln 2) \left(\frac{\lambda - \lambda_{F'F''}}{\Delta\lambda_{De}} \right)^2 \right]$$

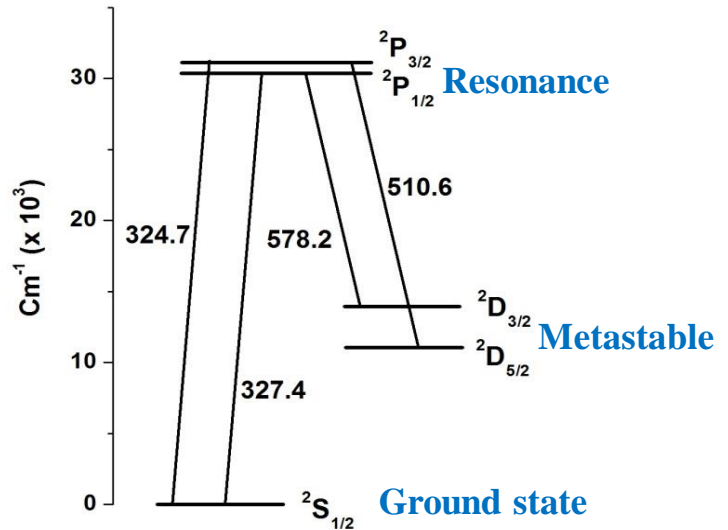
$$k(\lambda) = \frac{2}{\Delta\lambda_{Da}} \sqrt{\frac{\ln 2}{\pi}} \cdot k_0 \cdot \frac{1}{\sum_k (\rho_k \sum_{F'F''} S_{F'F''})} \times \sum_k \rho_k \sum_{F'F''} S_{F'F''} \text{Exp} \left[-4(\ln 2) \left(\frac{\lambda - \lambda_{F'F''}}{\Delta\lambda_{Da}} \right)^2 \right]$$

- Intensity of the transmitted light: $I^T = \int I(\lambda) \cdot \text{Exp}(-L \cdot k(\lambda)) d\lambda$
can no more be deduced from the equation given by Mitchell and Zemansky but must be calculated by numerical integration.

Calculated variation curves of I^T/I_0 of 327.4 nm line versus Cu density for different T_e , from which the measured absorption rate was converted to Cu density

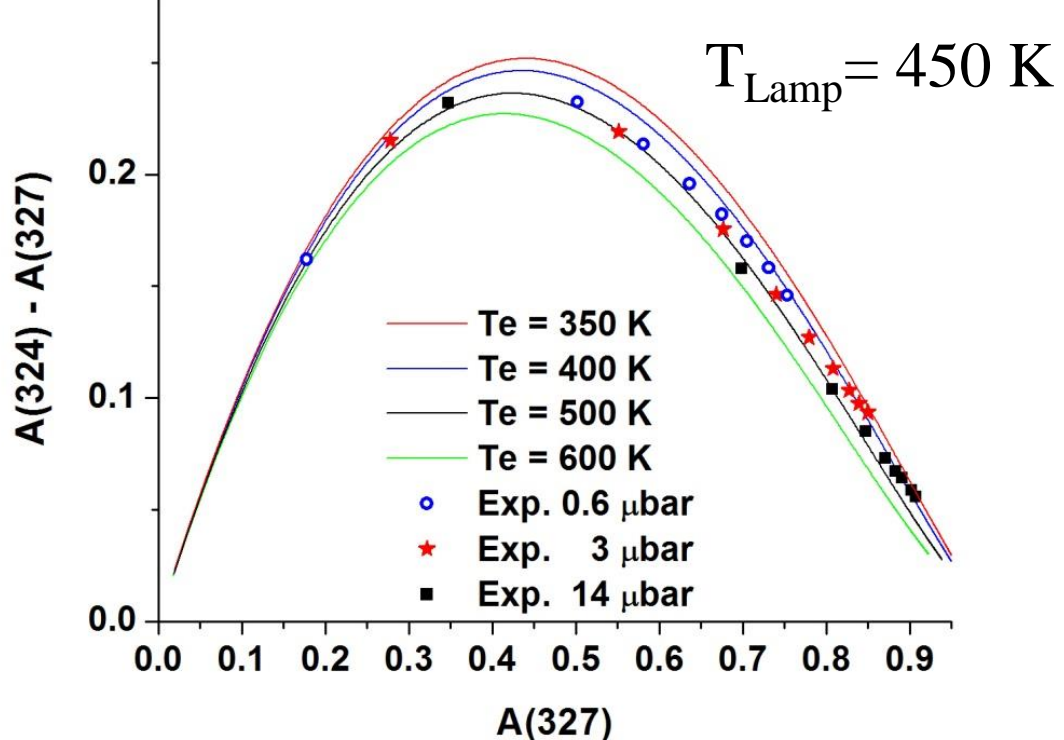


Determination of the gas temperature in the Hollow Cathode Lamp at $i=5$ mA



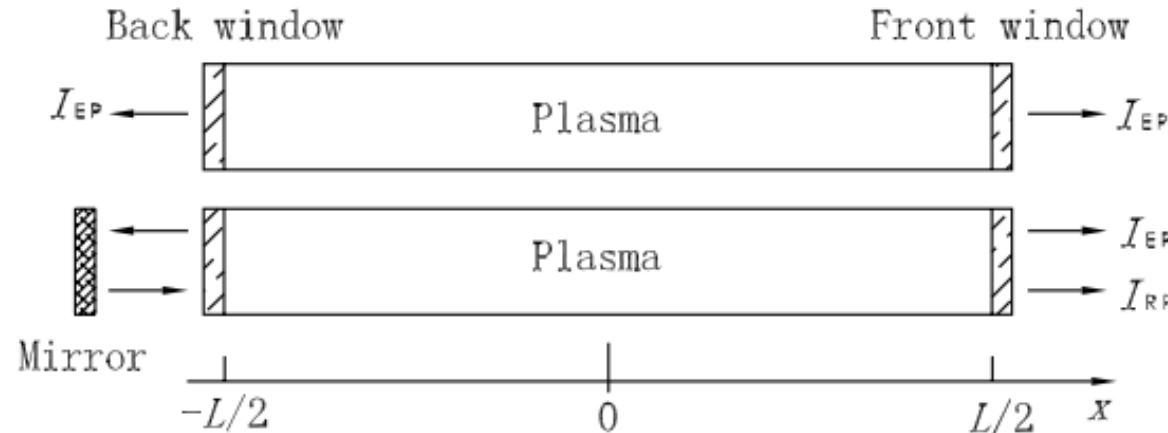
$$f_{327.4} = 0.220$$

$$f_{324.7} = 0.439$$



Difference in absorption rates of 324.7 and 327.4 nm lines versus the absorption rate of the 327.4 nm line. Theoretical curves are for 350, 400, 500 and 600 K (down from the top, respectively). Experimental data are for different magnetron discharge powers at 0.6, 3 and 14 μ bar.

Self absorption techniques



$$I_{EP}(\nu) = t_1 \int_0^L i(x, \nu) \exp\left[-\int_x^L \alpha(x', \nu) dx'\right] dx$$

$$I_E = \int_{-\infty}^{+\infty} I_{EP}(\nu) d\nu$$

$$I_{RP}(\nu) = rt_2^2 I_{EP}(\nu) \exp\left[-\int_0^L \alpha(x, \nu) dx\right]$$

$$I_R = \int_{-\infty}^{+\infty} I_{RP}(\nu) d\nu$$

The density of absorbing species is deduced from $\gamma = \frac{I_R + I_E}{I_E}$

γ depends on space distribution of emission and absorbing atoms density

Example: absorption on Ar metastable atoms in a CCP plasma

J. Phys. D: Appl. Phys. **46** (2013) 475205

Z-B Wang *et al*

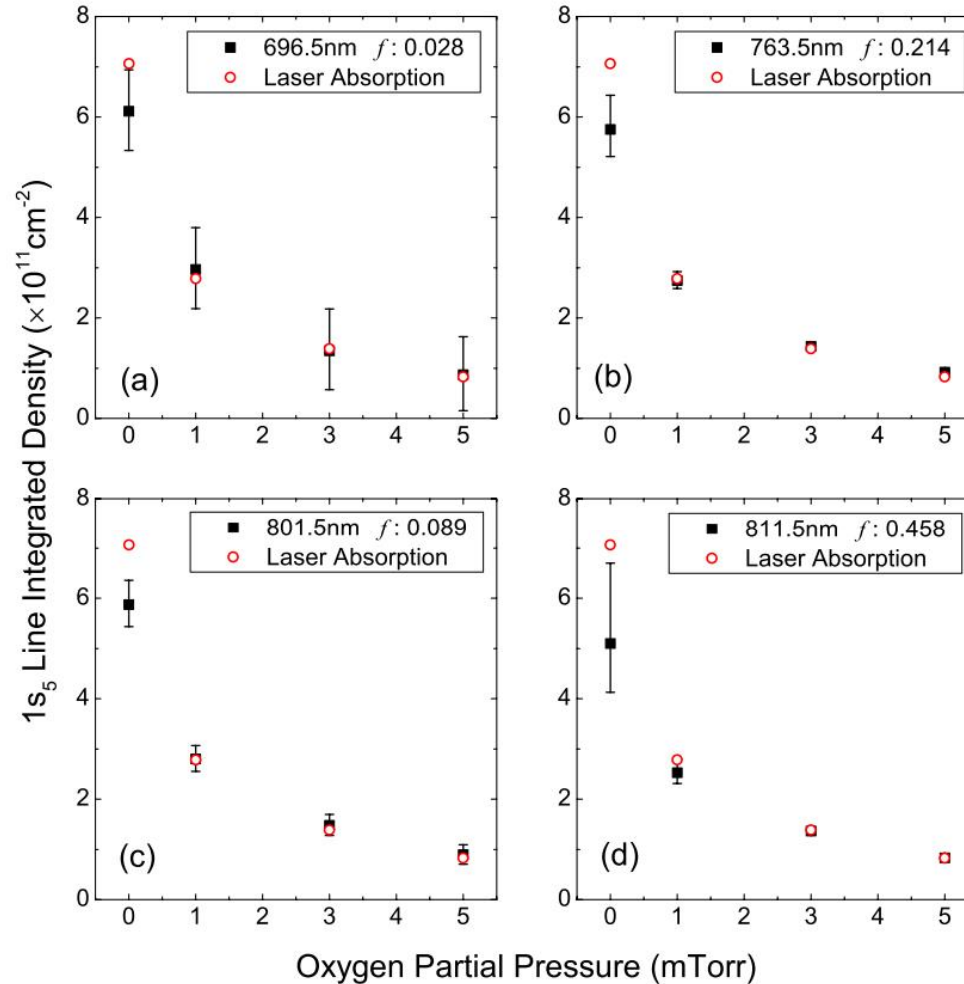
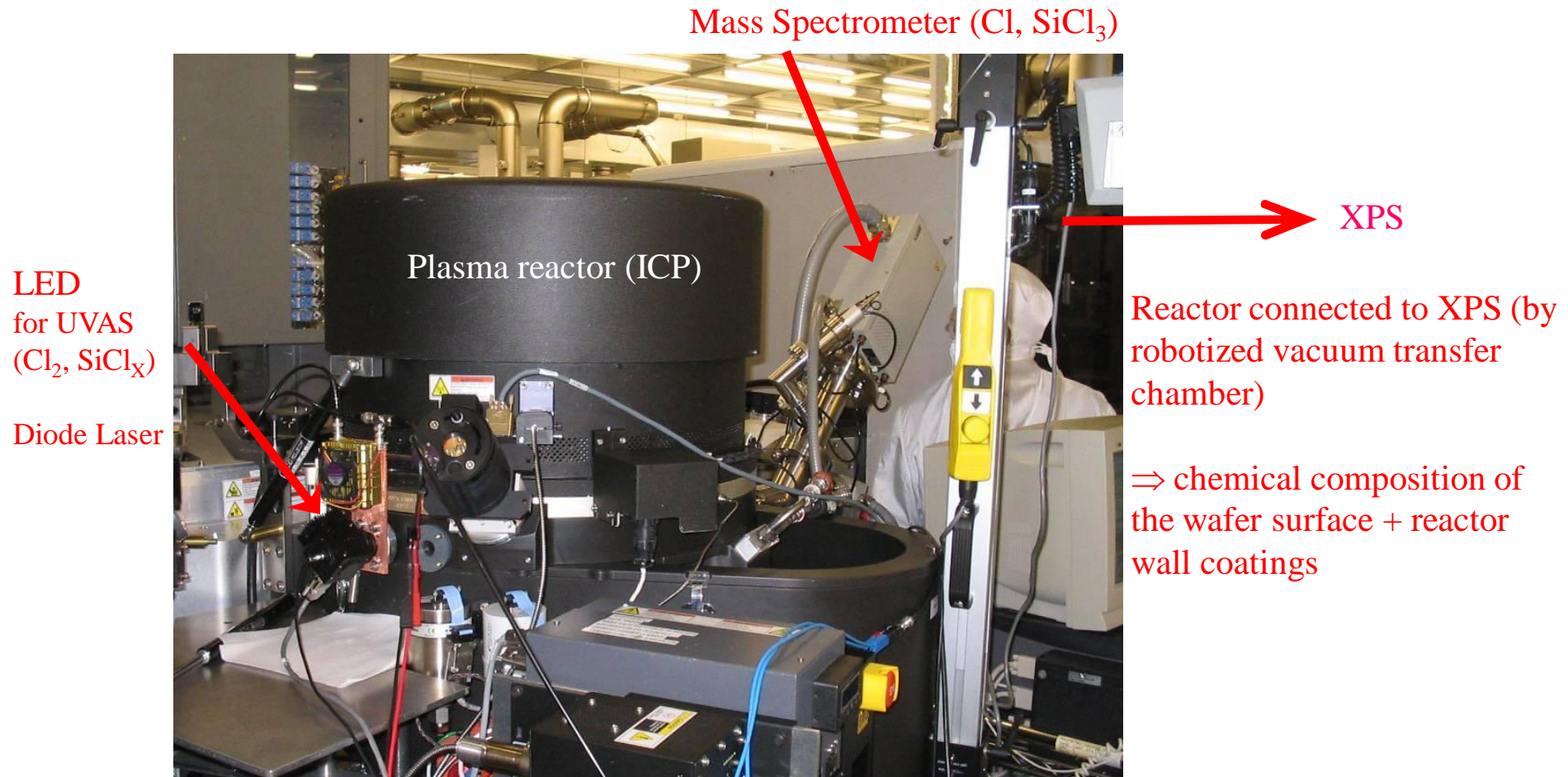


Figure 7. The measured line integrated density of $\text{Ar}^*(1s_5)$ atoms versus oxygen partial pressure by self-absorption and laser absorption. The relative error of laser absorption results is estimated to be less than 3%. The size of the error bars for the self-absorption data is obtained by considering the uncertainty in each of the measured quantities, including the intensity ratio γ , the effective reflection coefficient μ and the gas temperature T .

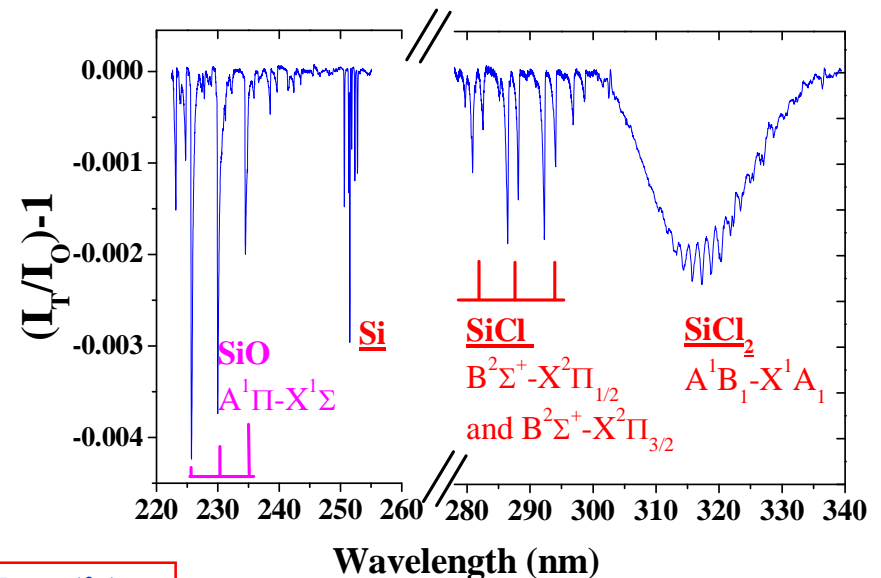
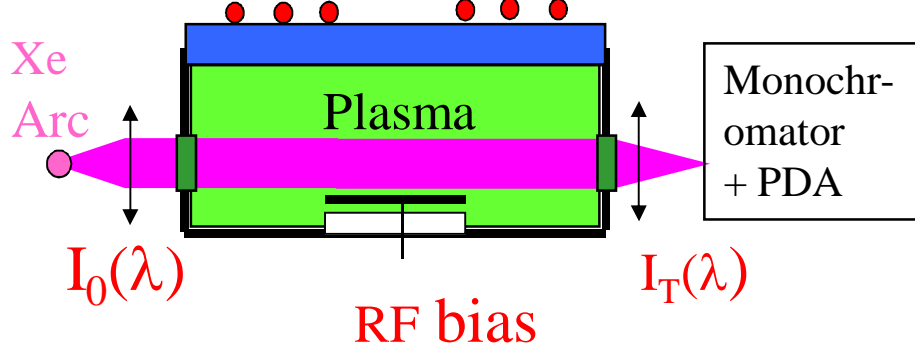
Broad-Band Absorption Spectroscopy (BBAS)

Experimental set-up

In LTM, we are using an industrial ICP reactor from AMAT designed to etch 300 mm wafers but modified to host plasma and surface diagnostics



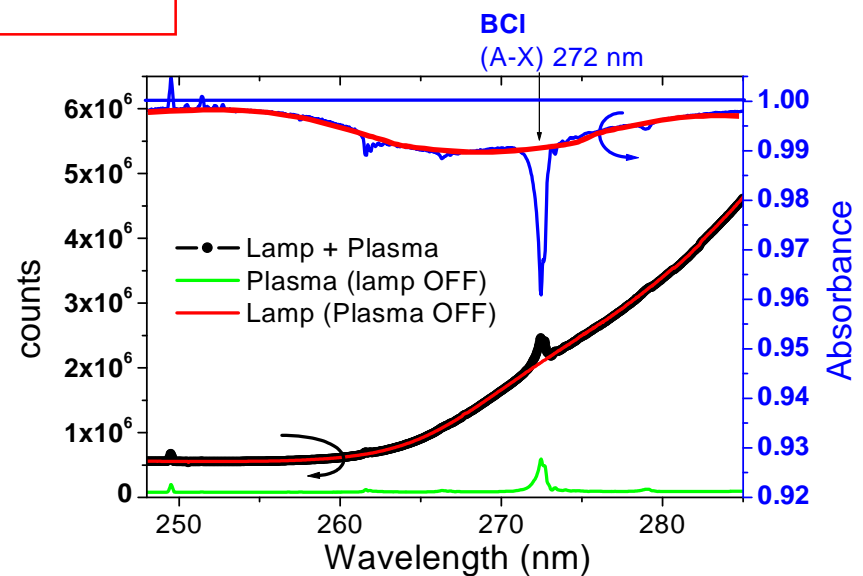
Radical density measurement by BBAS in Etch reactor



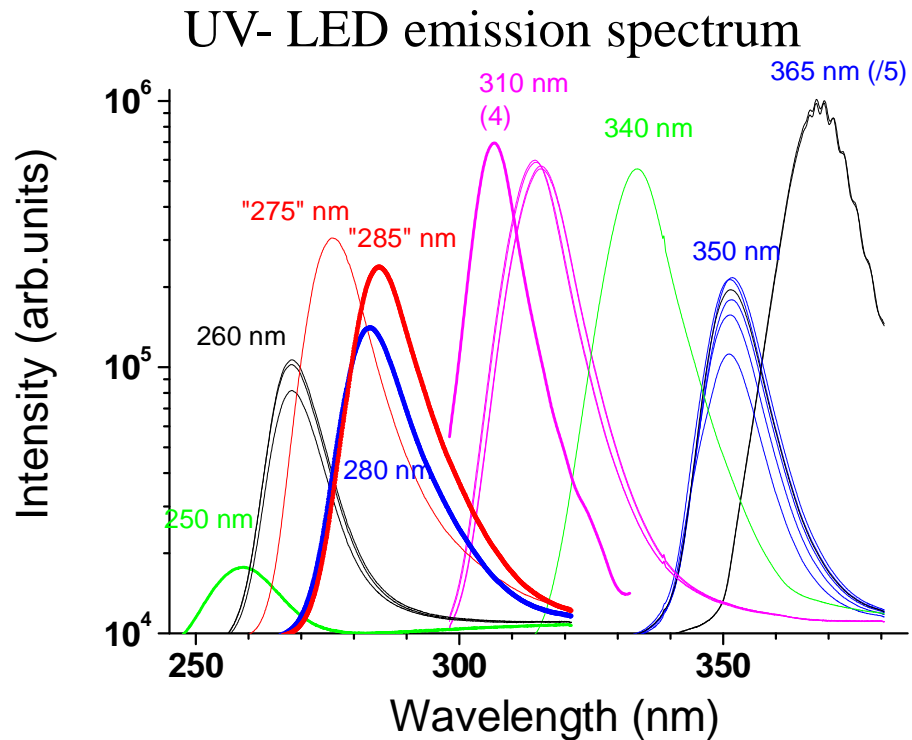
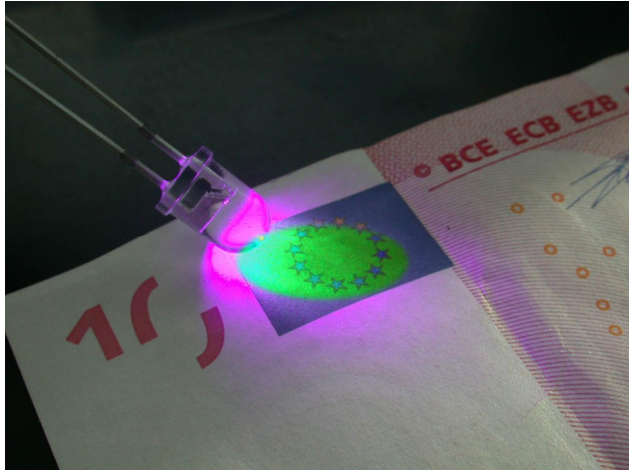
Beer-Lambert law: $I_T(\lambda) = I_o(\lambda) e^{-N \cdot L \cdot \alpha(\lambda)}$

By measuring $I_o(\lambda)$ and $I_T(\lambda)$: Radical density N

Note that absorbance $\approx 10^{-3} \Rightarrow$ high sensitivity
is required



Introduction of UV LEDs for high sensitivity absorption experiments



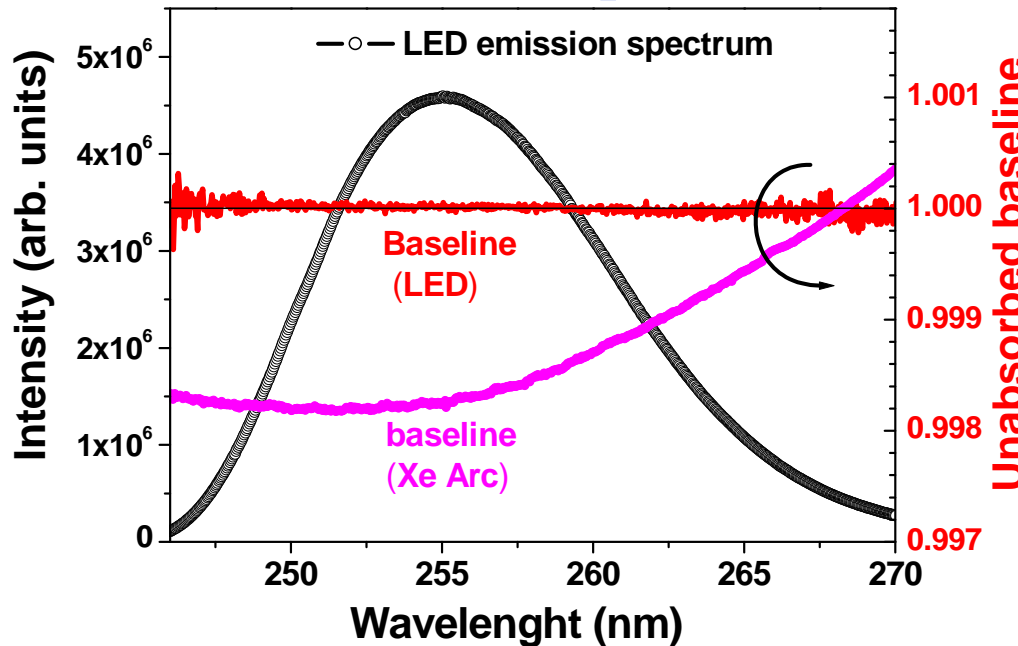
ÉLEDs cover the spectral range 240 nm ó 1500 nm with power > 200 µW

ÉEach diode has a spectral width of about 15 nm

ÉLEDs are solid state light sources: provide a very bright light point without intensity fluctuations when the LED is *thermoregulated* and fed by a stabilized current source

Stability characterization of a LED light source

To characterize the LED stability, 2 emission spectra are recorded with 5 minutes interval in vacuum (no absorption) and divided by each other



The LED emission intensity $I_0(\lambda)$ is highly stable, leading to flat baseline

Xe arc : sensitivity limited by baseline oscillations ($> 10^{-3}$)

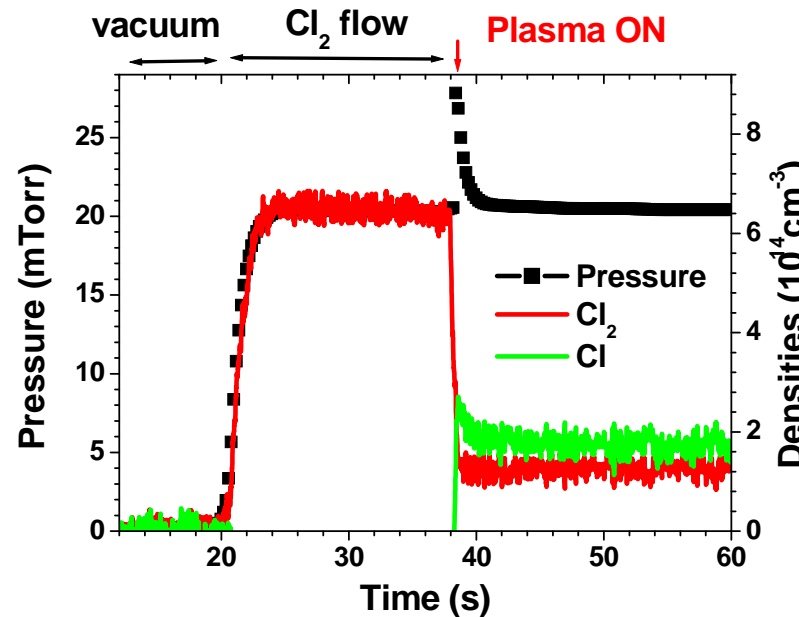
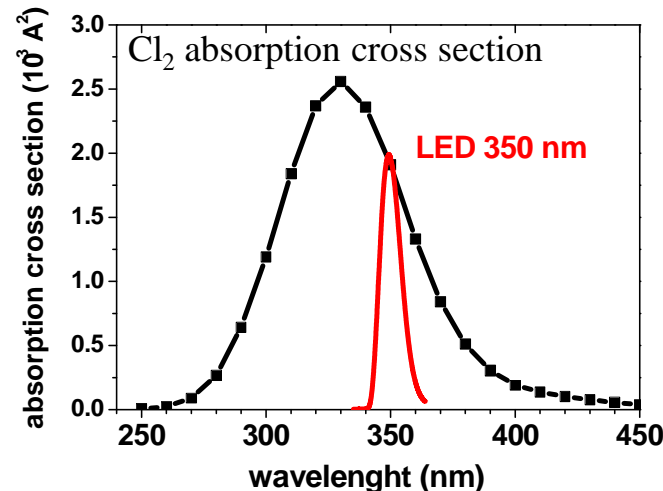
LED: sensitivity is limited by the baseline noise ($< 10^{-4}$)

⇒ we gain 1 order of magnitude in sensitivity !

BBAS with UV-LED for real time
process monitoring

Real time plasma monitoring: example of Cl₂

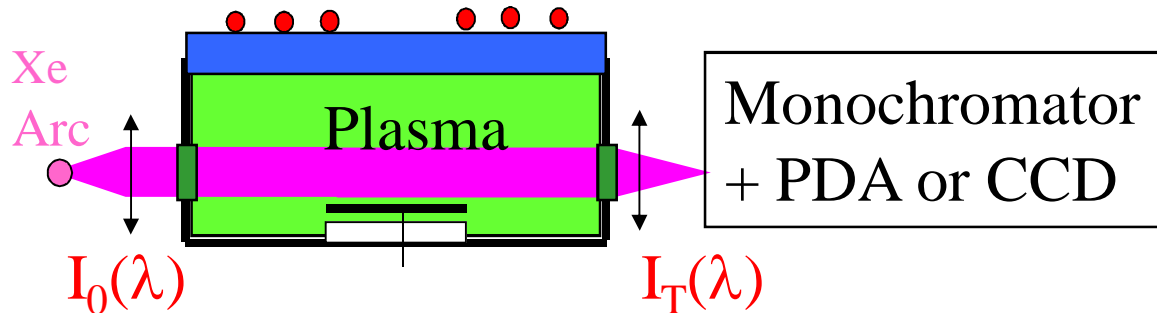
Cl₂ is detected with 350 nm LED Example: Cl₂ plasma *without wafer*



Plasma composition : 55 % Cl et 45 % Cl₂

⇒ Thanks to the lock-in, real time monitoring of radical density is possible with 10 ms resolution

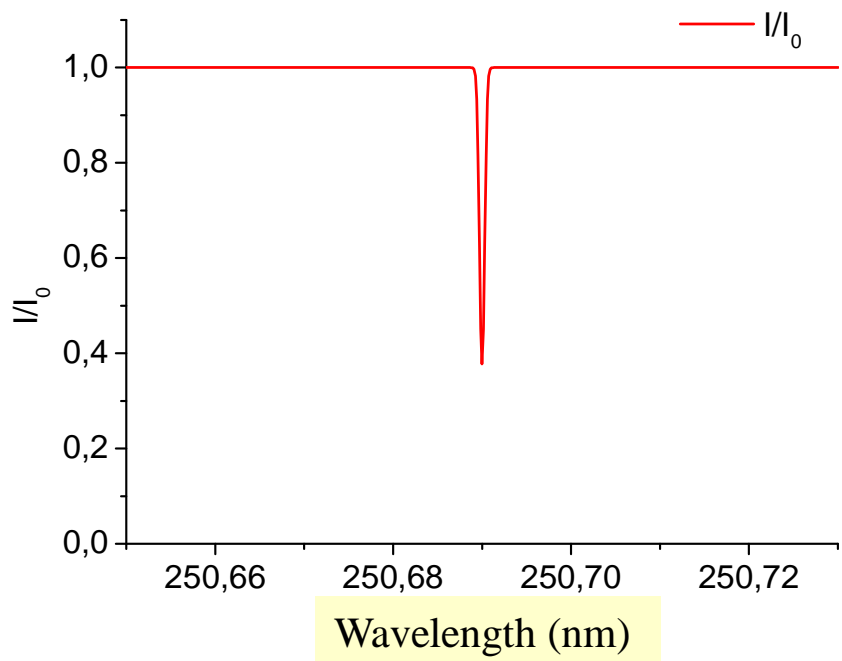
Artifact: Influence of instrumental spectral resolution in BBAS



**The real absorption profile
(with a very high resolution
Mono) would be:**

The density is calculated by:

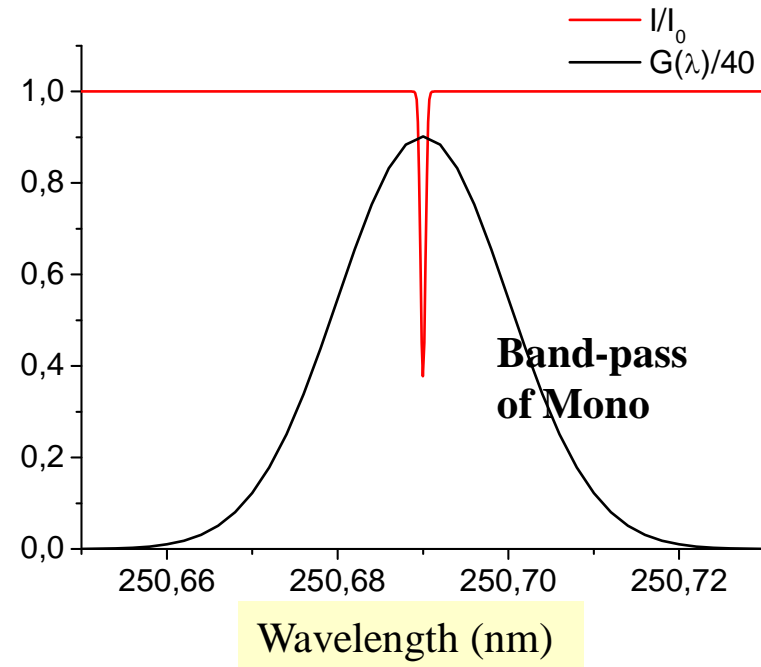
$$\langle N \rangle = \frac{K}{l} \cdot \int L n\left(\frac{I_0(\nu)}{I(\nu)}\right) d\nu$$



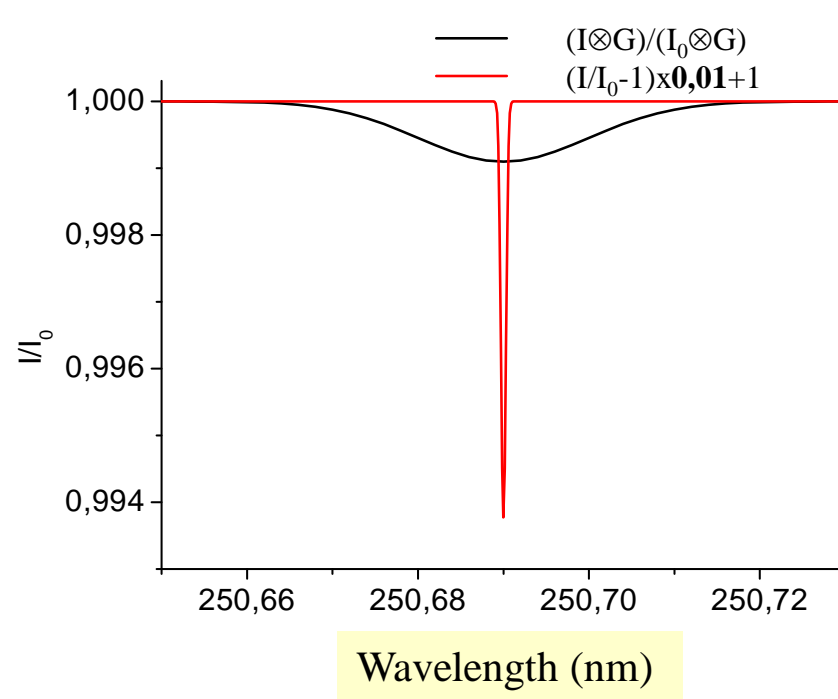
Recorded profiles in BBAS

In BBAS, the spectral resolution is provided by the monochromator. So both recorded I_0 and I have been convoluted with the spectral band-pass of the monochromator

Real profile

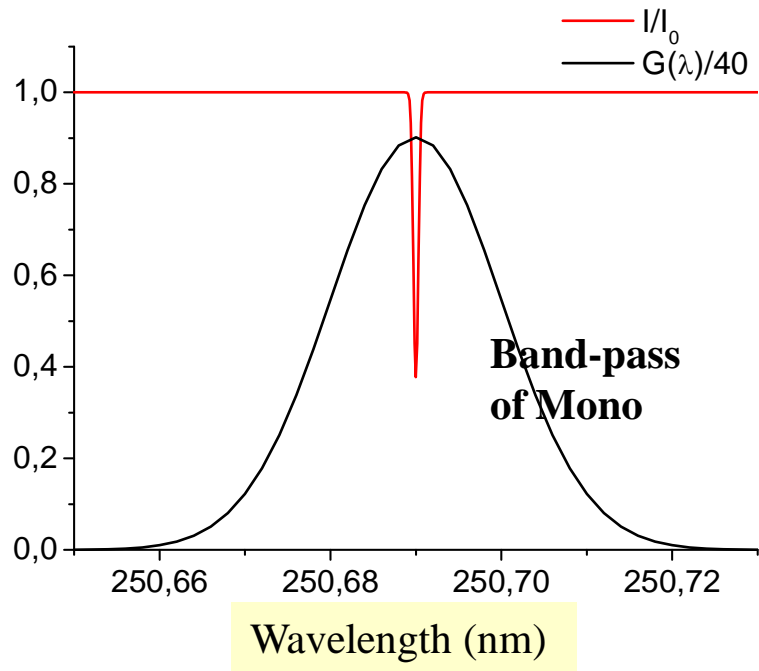


Recorded profile

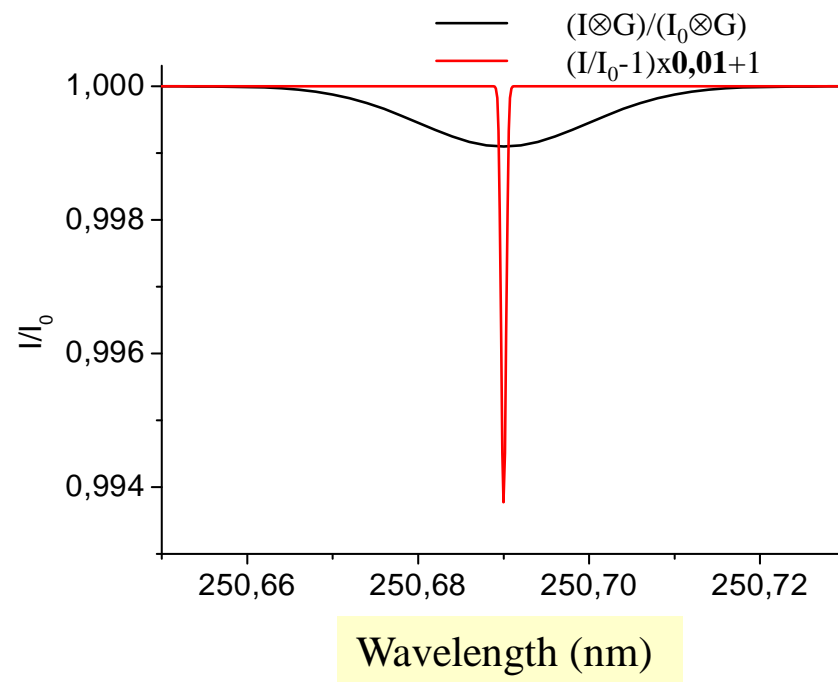


Recorded profiles in BBAS

Real profile



Recorded profile



Behind the monochromator.

$$\int \left(\frac{I_0(\lambda)}{I(\lambda)} \right) d\lambda \equiv \int \left(\frac{I_0(\lambda) \otimes G(\lambda)}{I(\lambda) \otimes G(\lambda)} \right) d\lambda$$

But: $\frac{K}{l} \int \ln \left(\frac{I_0(\lambda) \otimes G(\lambda)}{I(\lambda) \otimes G(\lambda)} \right) d\lambda$ Is not $\langle N \rangle = \frac{K}{l} \int \ln \left(\frac{I_0(\lambda)}{I(\lambda)} \right) \otimes G(\lambda) d\lambda$

Correct treatment of data in BBAS

What is conservative is the area under the absorption curve W

$$W = \int \left(1 - \frac{I(\lambda) \otimes G(\lambda)}{I_0(\lambda) \otimes G(\lambda)}\right) d\lambda \equiv$$
$$\int \left(1 - \frac{I(\lambda)}{I_0(\lambda)}\right) d\lambda = \int (1 - \exp(-\sigma(\lambda, T) N * L)) d\lambda$$

1- W is evaluated for different values of the density by taking into account the line profile and spectral resolution of the monochromator.

2- Density is deduced by the comparison of experimentally measured W and model curves.

J. Phys. D: Appl. Phys. 37 (2004) 1954

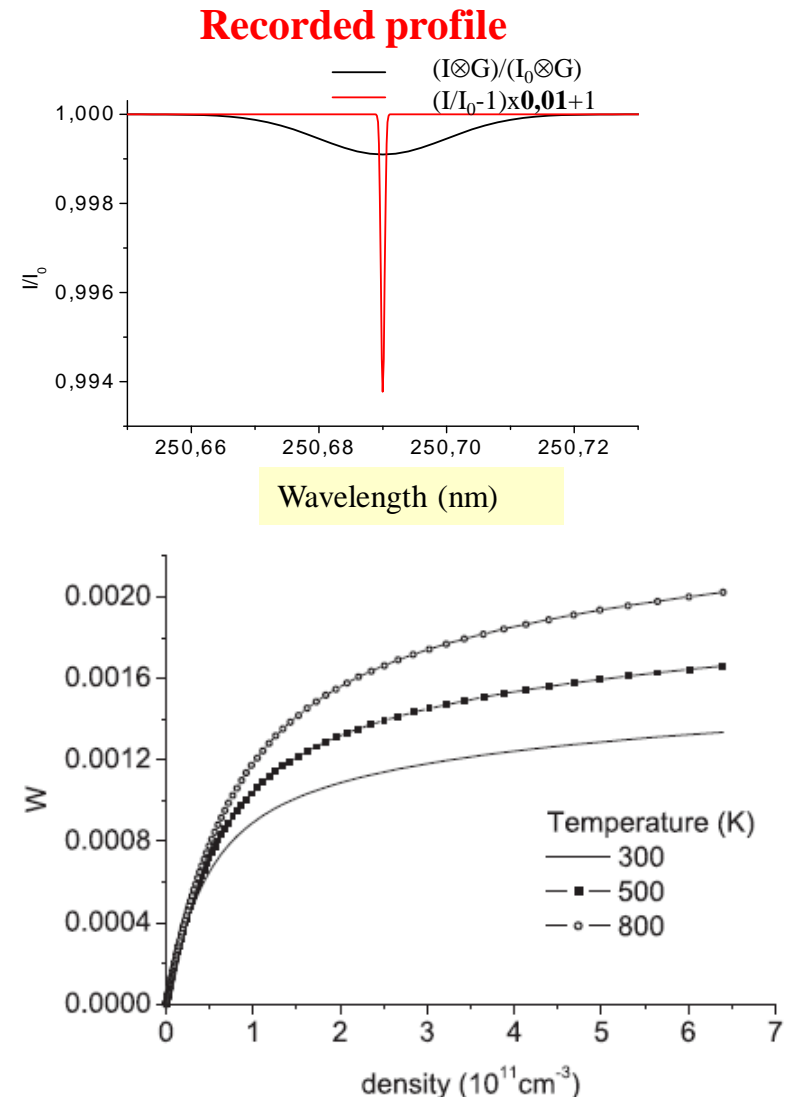
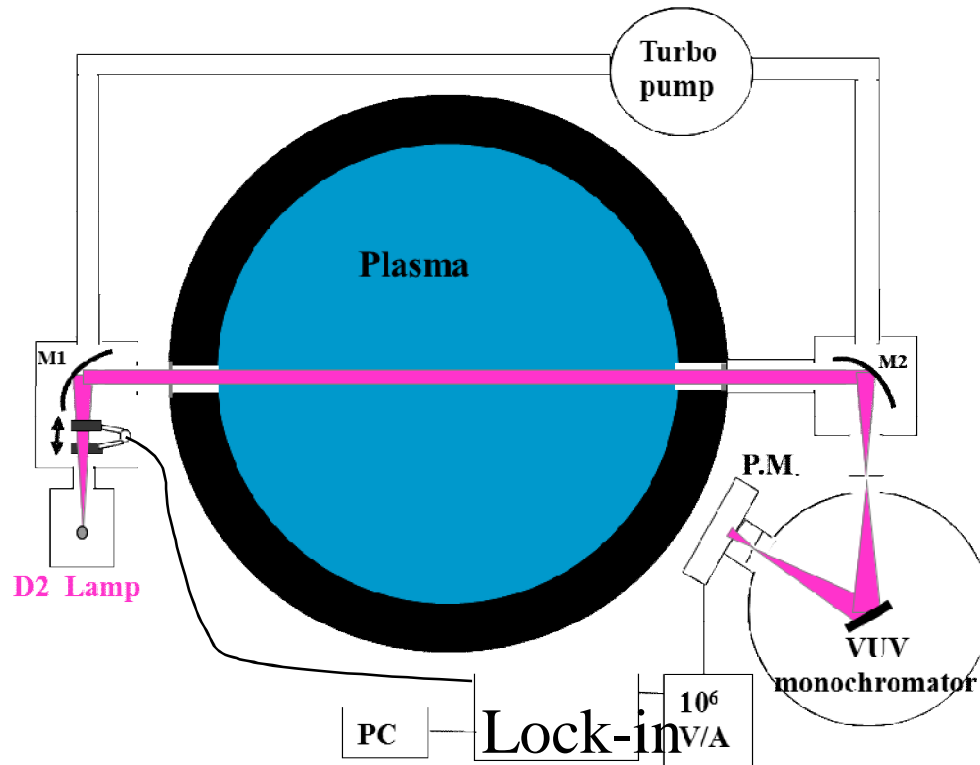


Figure 3. Density dependence of W with the temperature as parameter for the Si 250.69 nm line.

VUV BBAS: experimental set up (top view)

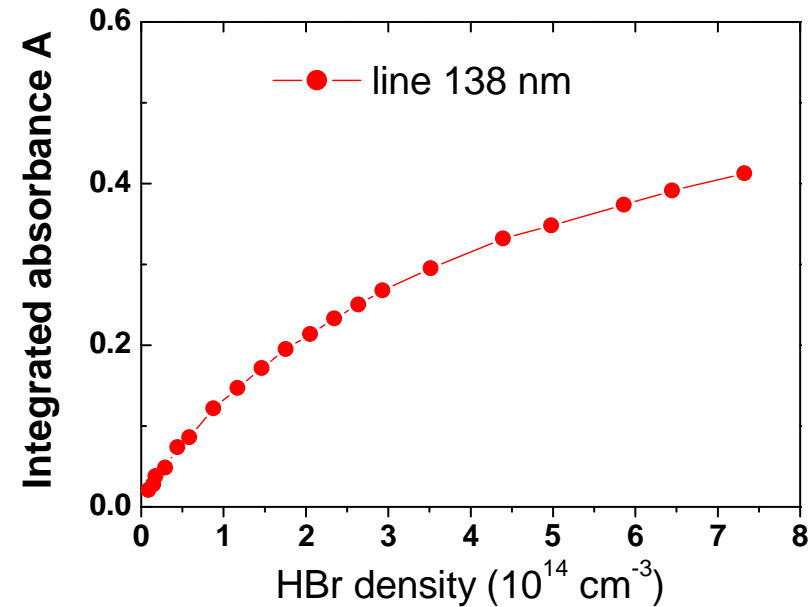
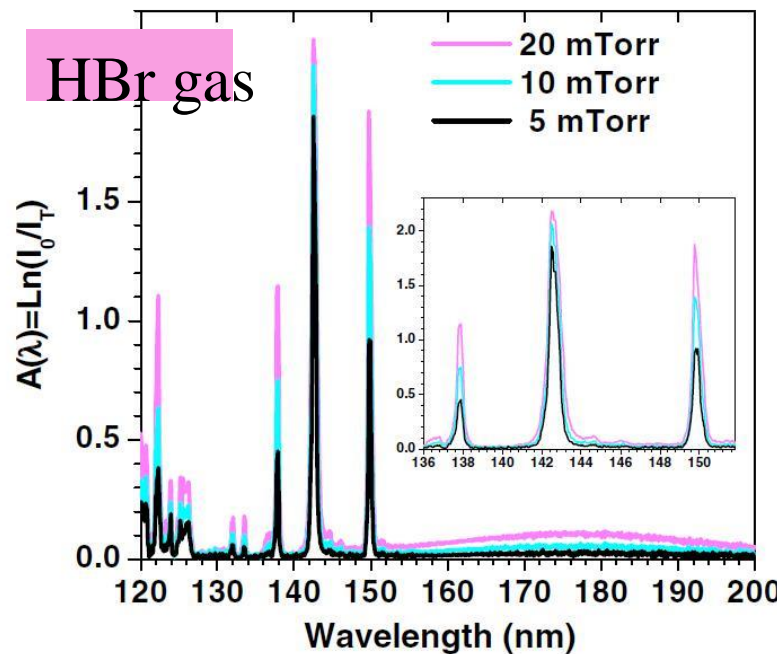
Specificity of the technique: optical path under vacuum + reflective optics (achromatic)



Acquisition system identical to UV-visible:
Species detected: HBr, Br₂, Cl₂, SiCl₄, BCl₃

BB-VUV absorption to detect closed shell molecules

Many *closed shell molecules* relevant for processing (HBr, Br₂, HCl, Cl₂, SiCl₄, CH₂F₂ etc) have strong absorbing bands toward Rydberg states in the VUV.



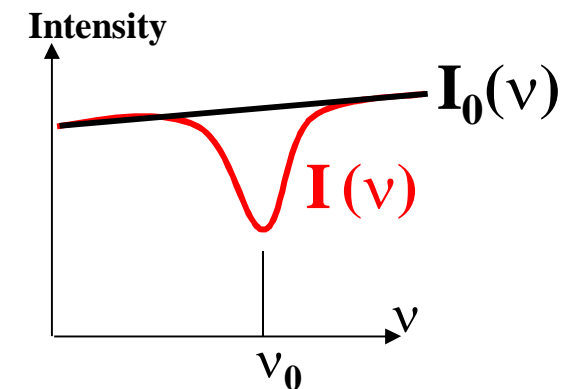
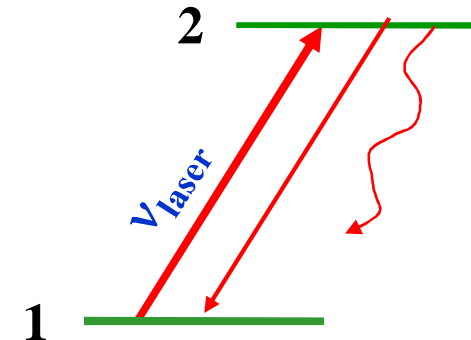
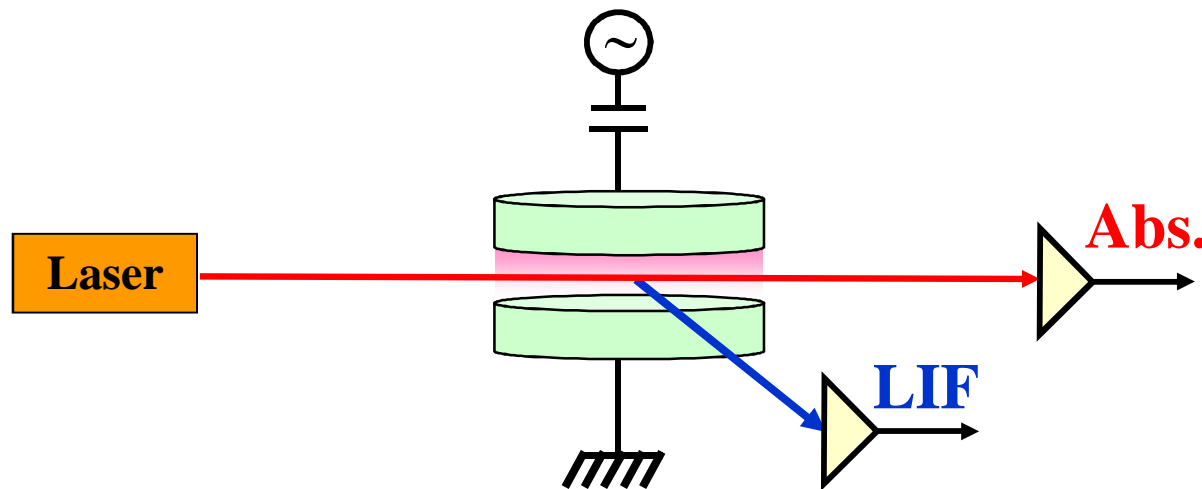
⇒ Very sensitive technique .but absorption is often saturated

This is not an issue for stable gases since relation absorbance/ density is calibrated from measurement without plasmas (i.e. for Cl₂, SiCl₄, HBr, etc)

Laser absorption techniques

Laser Absorption Spectroscopy

Laser frequency is tuned to a specific transition of the atom

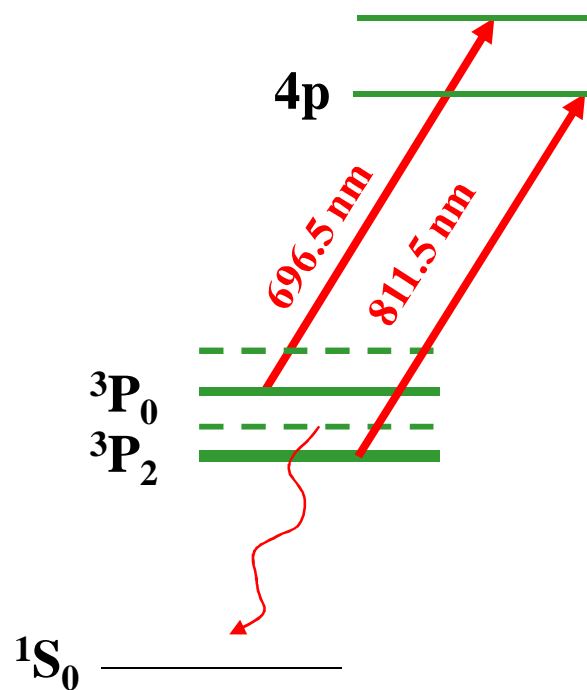


$$\ln\left(\frac{I_0(\nu)}{I(\nu)}\right) = l \cdot \alpha(\nu)$$

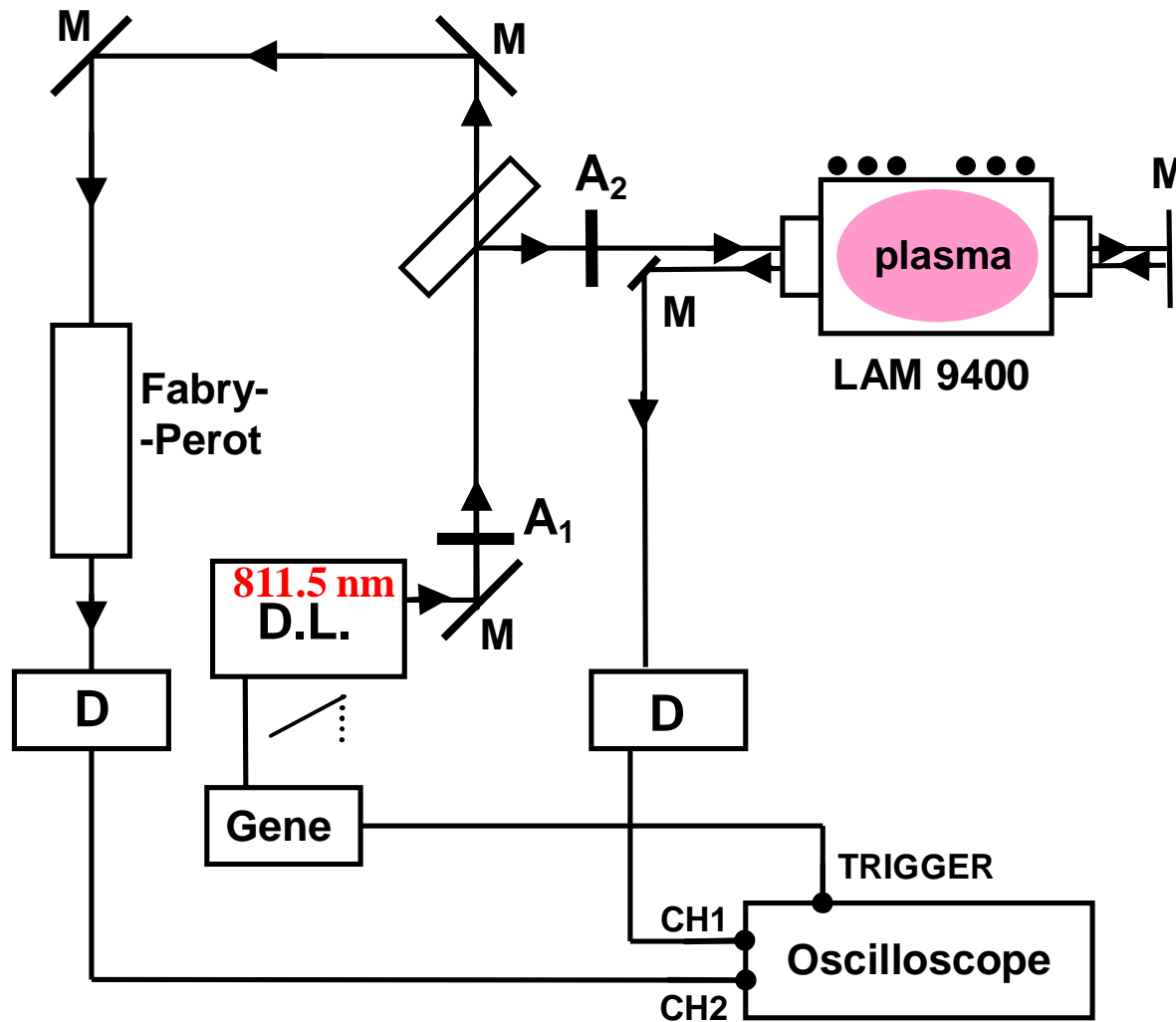
$$\alpha(\nu) = \frac{4hB_{12}}{\lambda\gamma} \left(n_1(\nu) - \frac{g_1}{g_2} n_2(\nu) \right)$$

Gas temperature in reactive plasmas

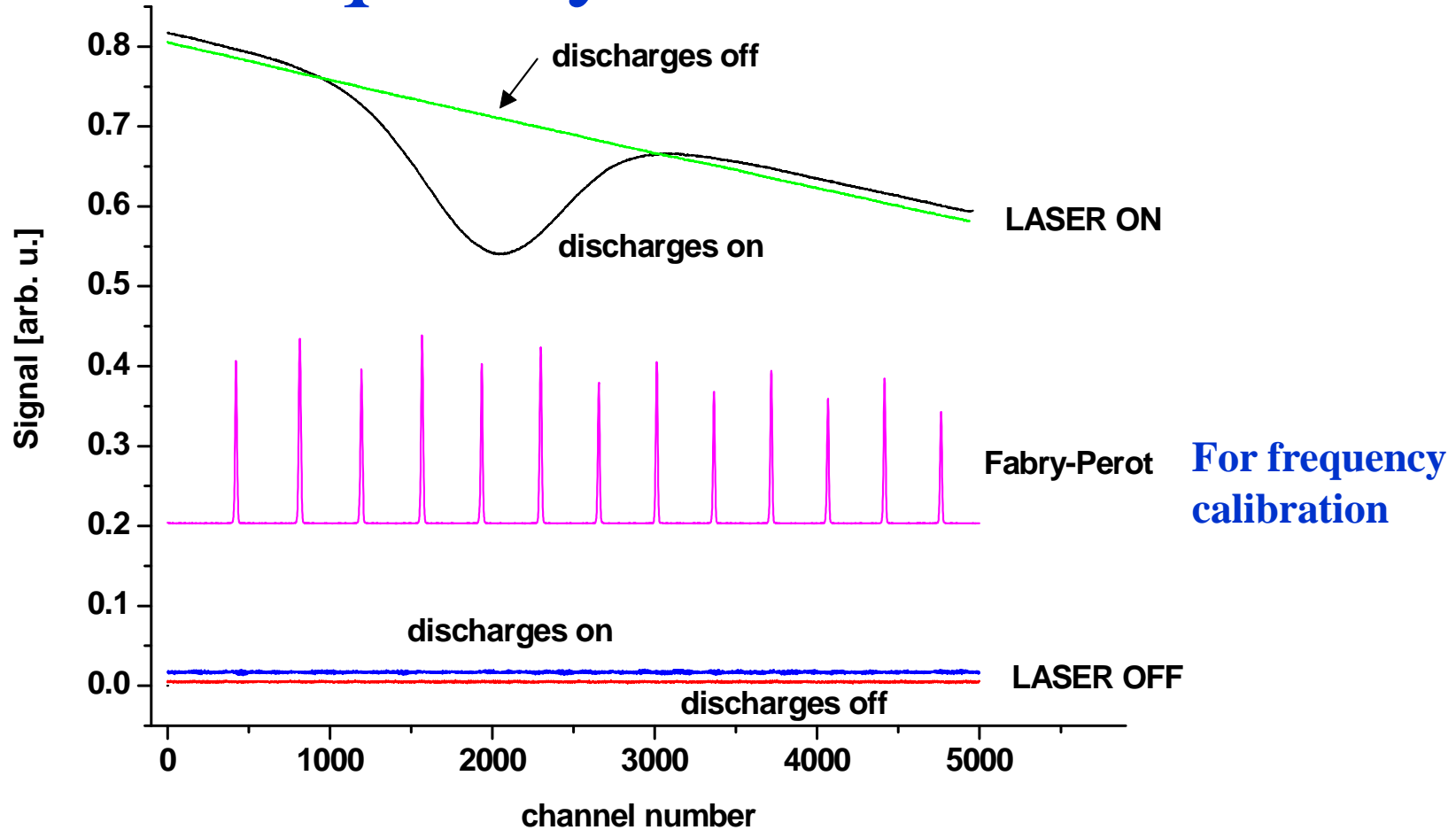
A few % of argon is added to the reactive plasma and the gas temperature is deduced from the Doppler profile of a line absorbed by atoms in the metastable state



Experimental set-up for Ar* absorption profile measurement (2)



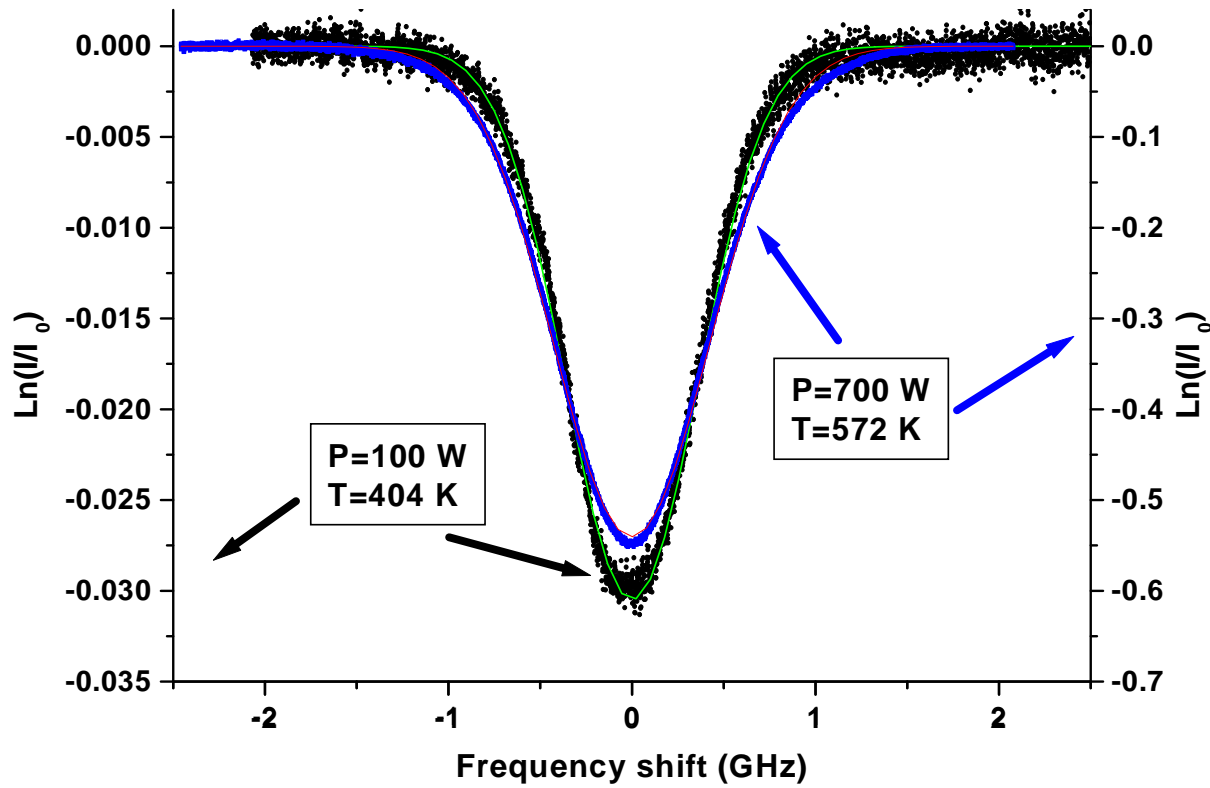
Recorded signals when the laser frequency is scanned



Determination of the Doppler width

$$I/I_0 = (S_{\text{laserON+dischargeON}} - S_{\text{laserOFF+dischargeON}}) / (S_{\text{laserON+dischargeOFF}} - S_{\text{laserOFF+dischargeOFF}})$$

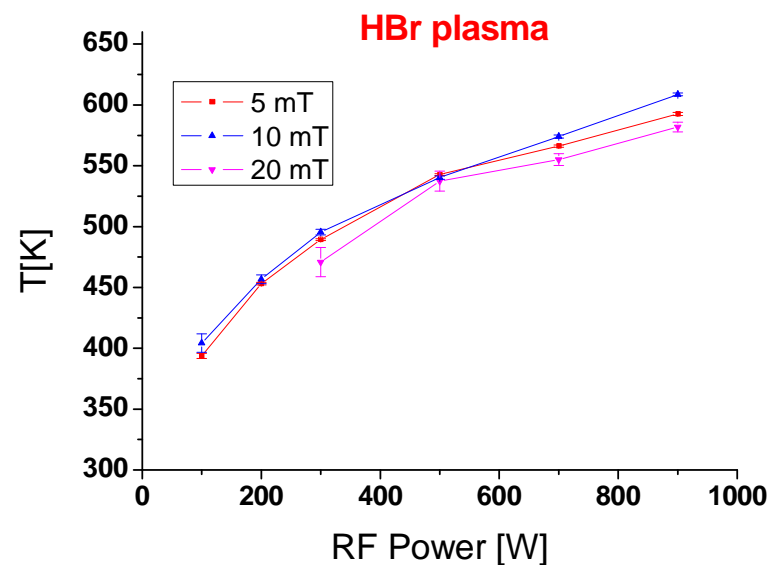
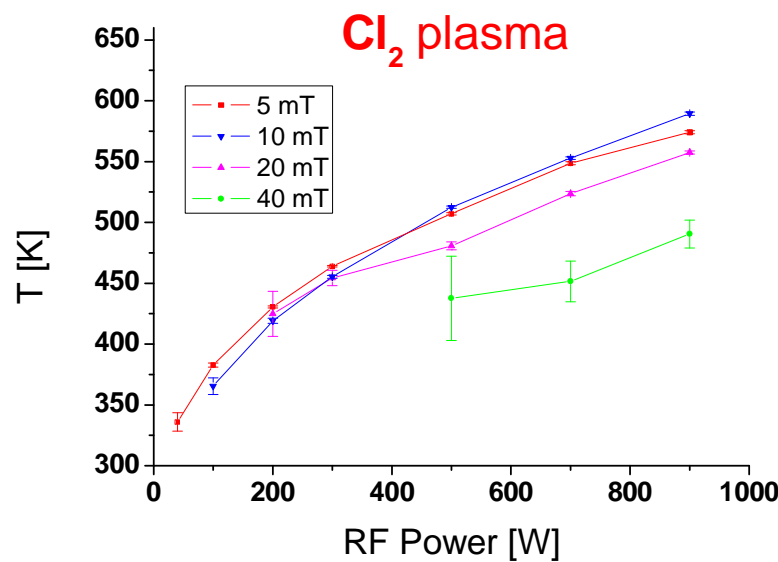
$\text{Cl}_2 + 10\% \text{ Ar}$
at 5 mTorr



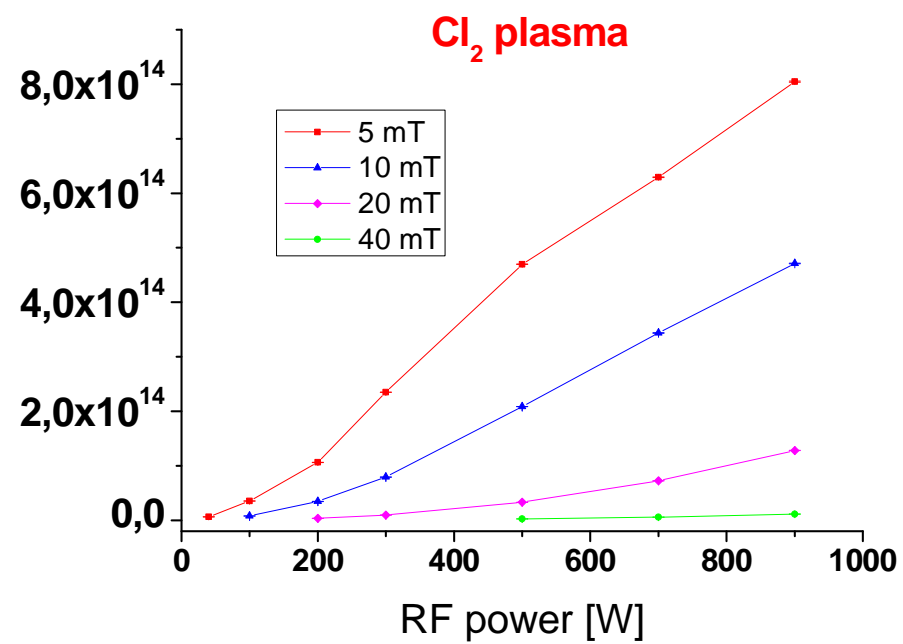
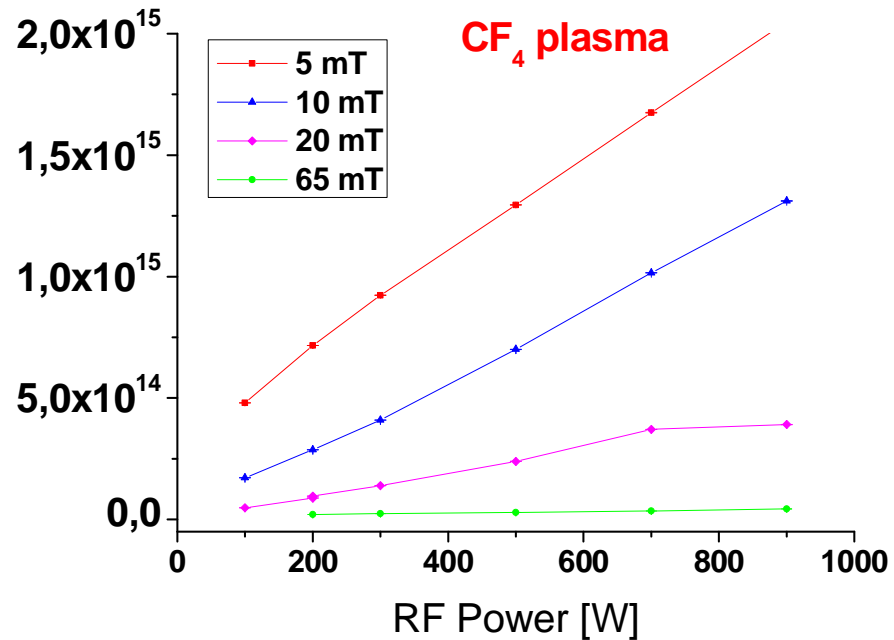
$$\delta\nu_D (\text{GHz}) = (2\nu_0 / c) \sqrt{2 \ln 2 (RT / M)} = 7.16 \cdot 10^{-16} \frac{c}{\lambda_0} \sqrt{T / M}$$

Results in HBr and Cl₂ plasmas (5 % of Ar)

(SiO₂ wafer without RF bias: no etching)



Result: Ar^{*}(³P₂) density

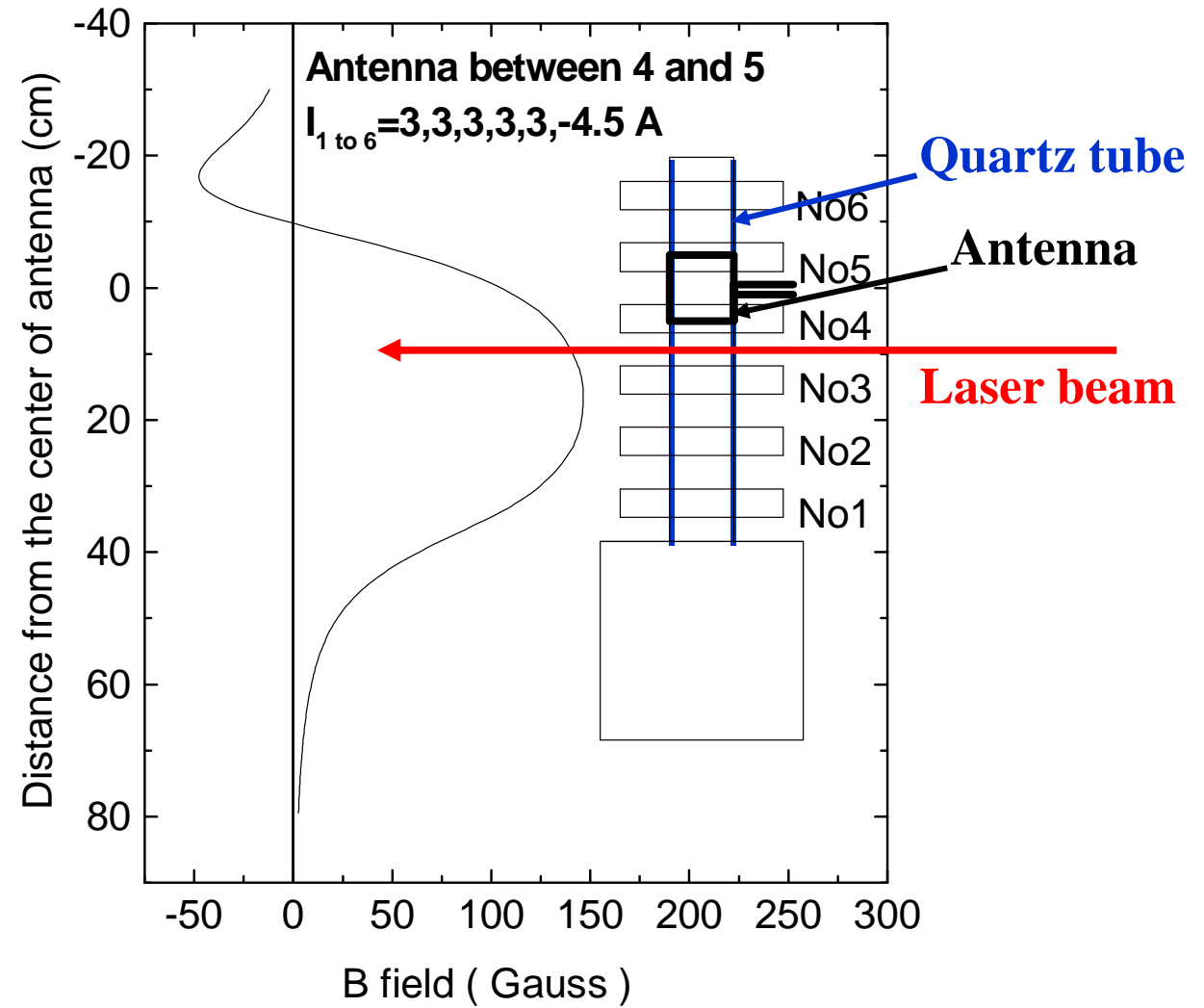


At 100 W, the density of Ar^{*}(³P₂) is 15 times smaller in Cl₂ than in CF₄ because k_q(Cl₂) = 71 x 10⁻¹⁷ m³.s⁻¹ et k_q(CF₄) = 4 x 10⁻¹⁷ m³.s⁻¹ (quenching)

see J.E. Velazco *et al*, J. Chem. Phys. **68** (1978) 4357

At high P_{RF}, Cl₂ is dissociated and k_q(Cl) < k_q(Cl₂) hence [Ar*] increases

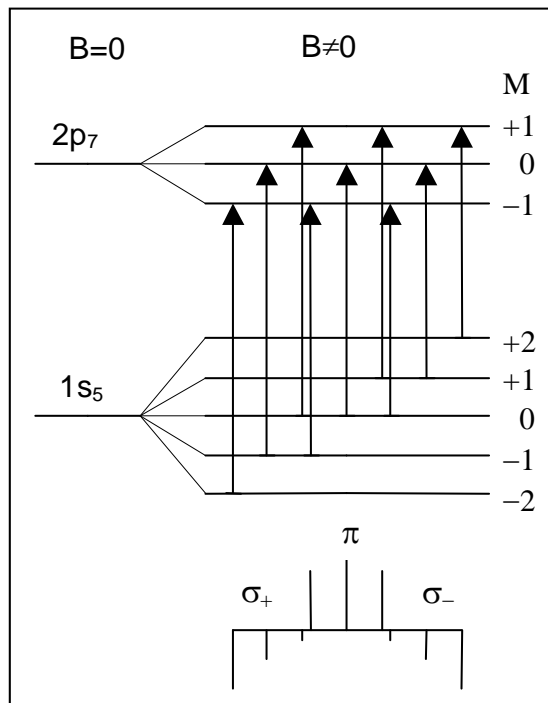
Line profile in presence of strong magnetic field in a low power Helicon Argon plasma; p= 0.9 to 10 μ bar



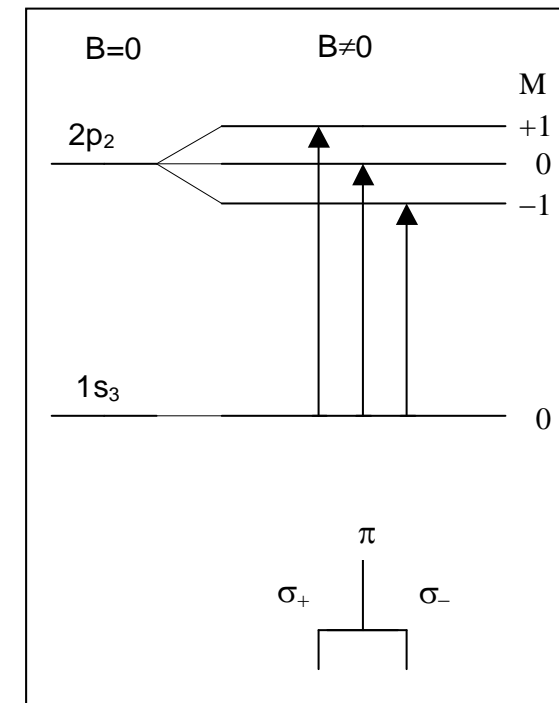
Line profile in presence of strong magnetic field

Zeeman components of the absorbing lines of Argon

722.38 nm; $2p_7 \leftarrow ^3P_2$ line



722.42 nm; $2p_2 \leftarrow ^3P_0$ line



$$\vec{k} \perp \vec{B}$$

if $\vec{E} \perp \vec{B}$ only σ^+ and σ^- lines exist

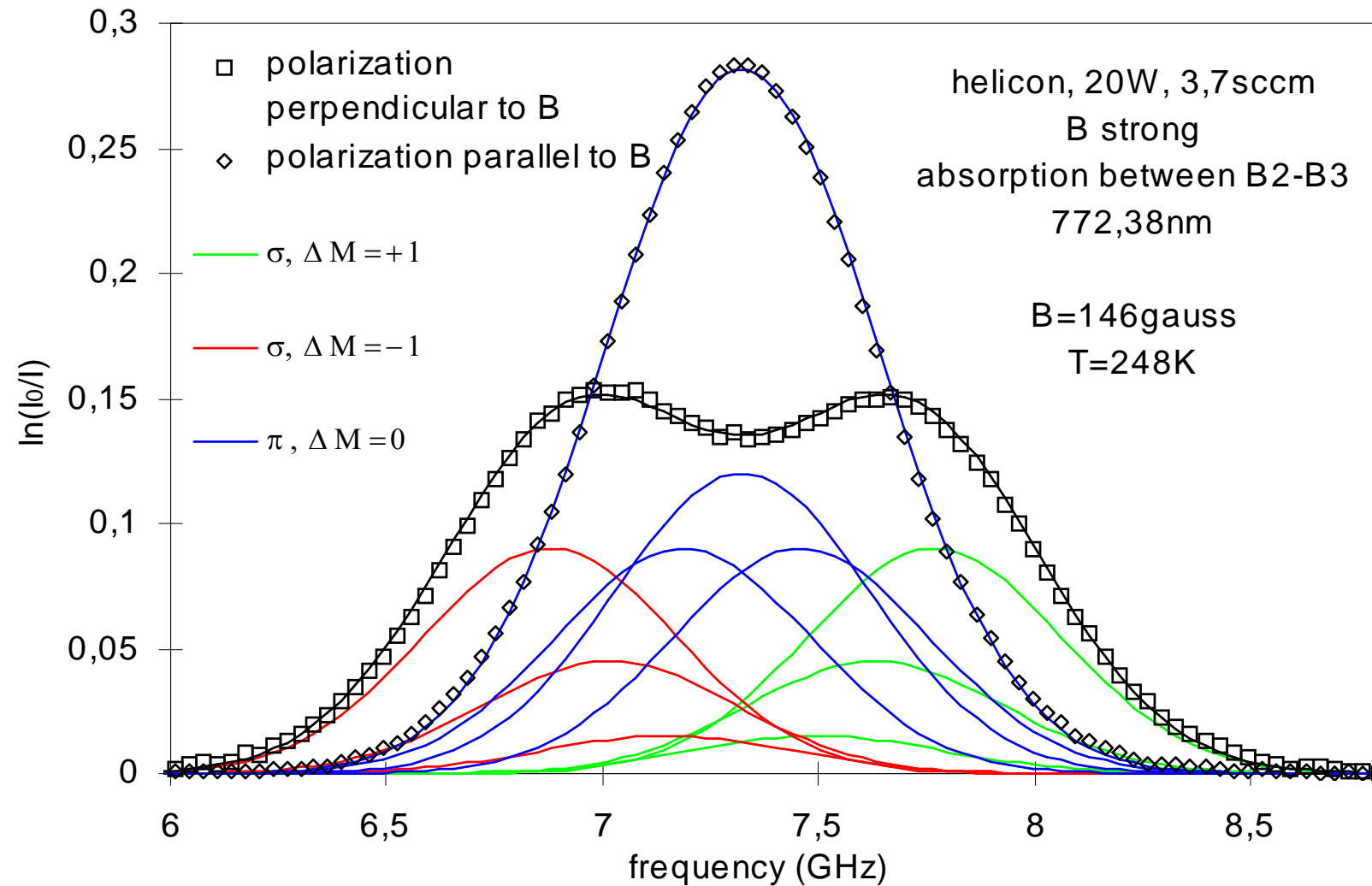
$$\vec{k} \perp \vec{B}$$

if $\vec{E} \parallel \vec{B}$ only π line (s) exist

$$\vec{k} \parallel \vec{B}$$

then only σ^+ and σ^- lines exist

Experimental profiles of the 722.38 nm line with two different polarization fitted with Gaussians



Equipement commun du Réseau Plasmas Froids

"Système Laser à Diode"

acquis sur les crédits MRCT ó CORTECH

Total des crédits reçus (2004-2007): 49551 p

- Responsables : Nader Sadeghi (LSP, Grenoble), dépositaire

E-mail: nader.sadeghi@ujf-grenoble.fr

Stéphane Mazouffre (ICARE, Orléans)

E-mail: stephane.mazouffre@cnrs-orleans.fr

- Matériel: lasers avec cavité externe du type Littrow et du type DFB fournissant qqs 10 mW continus dans une largeur spectrale d'environ 10 MHz ($\cong 10^{-5}$ nm)

- Fournisseur: TOPTICA, représenté par OLI

DL avec cavité externe acquis par RPF

Ces DL avec cavité externe (Littrow) sont balayables sur environ une vingtaine de GHz sans saut de mode (ssm). L'accord en longueur d'onde sur la gamme de fonctionnement est obtenu en changeant la température de la DL.

É 1 Électronique de commande (Sys DL 100/19), avec: contrôle de courant, contrôle de température et tiroir de modulation (géné de fréquence).

É 5 Têtes laser:

6 396 ó 399 nm;	10 mW;	20 GHz (ssm)	Ti, Al
6 402 ó 407 nm	10 mW	20 GHz (ssm)	Ga
6 652 ó 662 nm;	30 mW;	20 GHz (ssm)	H*
6 750 ó 791 nm;	30 mW;	30 GHz (ssm)	Ar*, O*
6 1059 ó 1090 nm;	30 mW;	15 GHz (ssm)	He*, N ₂ *

DL du type DFB acquis par RPF

Ces DL sont sans cavité externe mais ont un réseau de Brag intégré. Leur domaine d'accordabilité n'est que d'environ 1 nm. Le balayage en fréquence peut être obtenu par le courant (environ 20 GHz ssm) ou par la température (très lent <Hz mais sur toute la gamme: environ 1 nm \approx 1000 GHz ssm). La stabilité en fréquence n'est que \approx 200 MHz sur quelques minutes (\approx 20-50 MHz pour DL Littrow) mais convient pour raies élargies à haute pression.

**Él Électronique de commande (Sys DL- DFB 100/19), avec:
contrôle de courant, contrôle de température et tiroir de
modulation (géné de fréquence).**

É2 Têtes laser:

- | | | | |
|-------------------|--------|--------------|-----|
| 6 772 ó 773 nm; | 70 mW; | 20 GHz (ssm) | Ar* |
| 6 1081 ó 1083 nm; | 70 mW; | 20 GHz (ssm) | He* |

Matériels d'accompagnement:

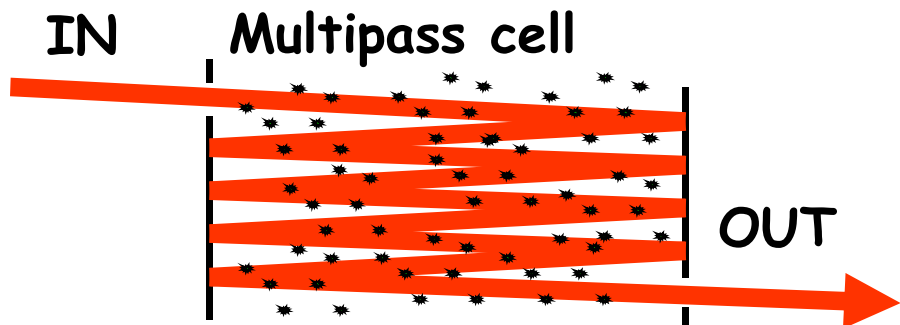
- É 1 Barreau en verre de 10 cm avec faces parallèles polies pour servir d'étaⁿon Fabry-Perot ayant un intervalle spectral libre de l'ordre de 1 GHz
- É 1 Lambdamètre devant permettre la mesure de longueur d'onde avec une précision de 3 pm. L'injection par une fibre optique monomode pose toujours quelques problèmes.
- É 3 photodiodes; sensibilité $\approx 1V/\mu W$; bande passante 15 kHz

High Sensitivity Absorption techniques

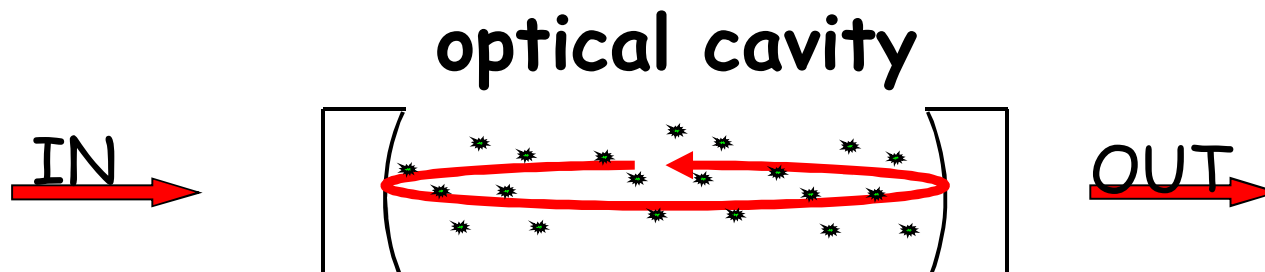
How is it possible to increase the sensitivity

* improving the detection limit ($\Delta I/I$):
Limited by the acquisition time and quality of detector

* With a multipass cell:
Hardly exceeds ~ 100



* With an optical cavity:
Possible only with laser sources. Number of passes can reach ~ 10000



< 2000 ICLAS

High sensitivity intracavity laser spectroscopy: applications to the study of overtone transitions in the visible range

A. CAMPARGUE, F. STOECKEL and M. CHENEVIER

Laboratoire de Spectrométrie Physique,* Université Joseph Fourier de Grenoble, B.P. 87, 38402 Saint-Martin-d'Hères Cedex, France

1988 Pulsed-CRDS

A. O'Keefe and D. A. G. Deacon, *Rev. Sci. Instrum.* **59**, 2544 (1988).



10 January 1997

1996 CW-CRDS

Chemical Physics Letters 264 (1997) 316–322

CW cavity ring down spectroscopy

D. Romanini, A.A. Kachanov, N. Sadeghi, F. Stoeckel

Laboratoire de Spectrométrie Physique–CNRS UMR 5588, Université J. Fourier – Grenoble I, B.P. 87 – 38402 Saint Martin d'Hères Cedex, France

CHEMICAL
PHYSICS
LETTERS

Received 25 September 1996; in final form 19 October 1996

2005 OF-CEAS

Appl. Phys. B 85, 397–406 (2006)

DOI: 10.1007/s00340-006-2356-1

Applied Physics B

Lasers and Optics

E.R.T. KERSTEL^{1,*}
R.Q. IANNONE¹
M. CHENEVIER²
S. KASSI²
H.-J. JOST^{3,*}
D. ROMANINI²

A water isotope (^2H , ^{17}O , and ^{18}O) spectrometer based on optical feedback cavity-enhanced absorption for in situ airborne applications

¹ Department of Physics, Center for Isotope Research, University of Groningen

2006 ML-CEAS

J. Phys. D: Appl. Phys. 37 (2004) 2408–2415

PII: S0022-3727(04)81448-7

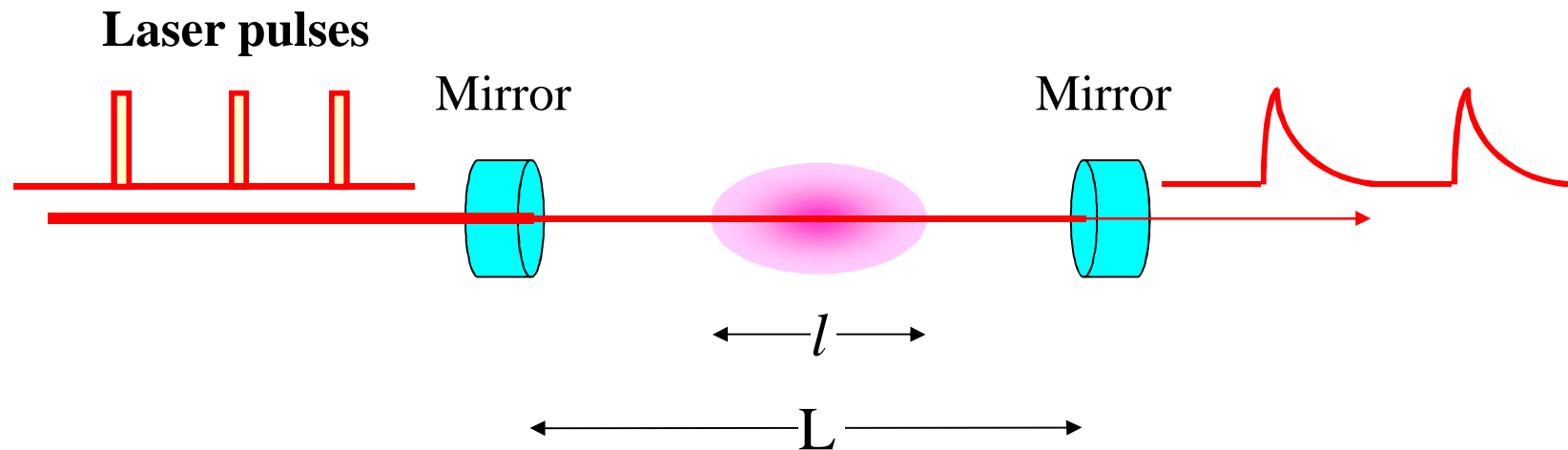
High sensitivity broad-band mode-locked cavity-enhanced absorption spectroscopy: measurement of $\text{Ar}^*(^3\text{P}_2)$ atom and N_2^+ ion densities

T Gherman, E Eslami, D Romanini, S Kassi, J-C Vial and
N Sadeghi¹

Cavity RingDown Spectroscopy (CRDS)

Using a pulsed laser

How it works?

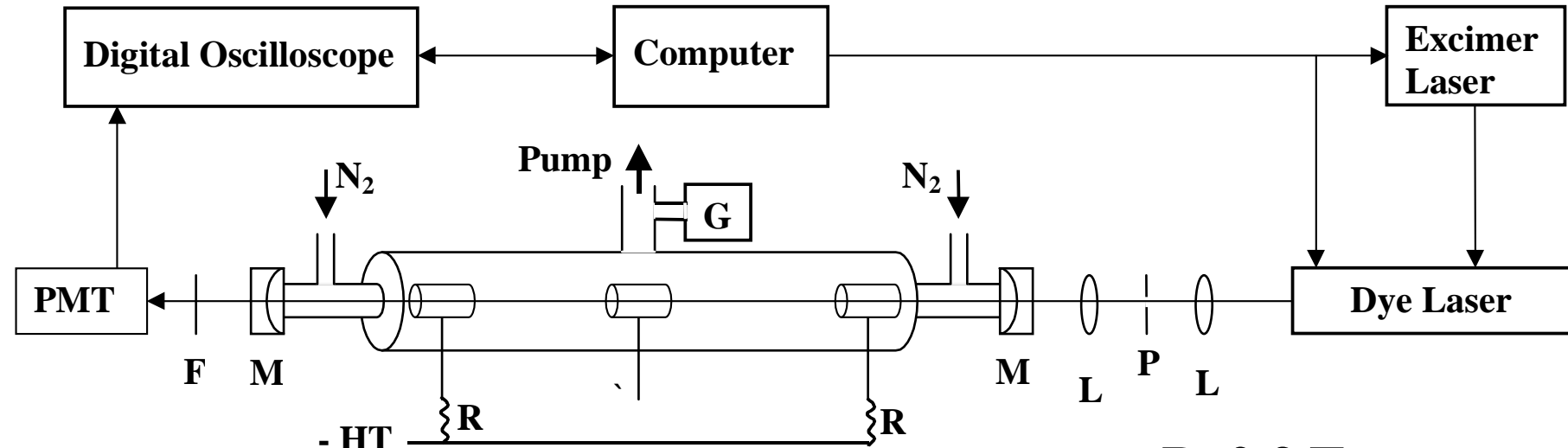


The decay rate of the intensity leaking from the cavity is:

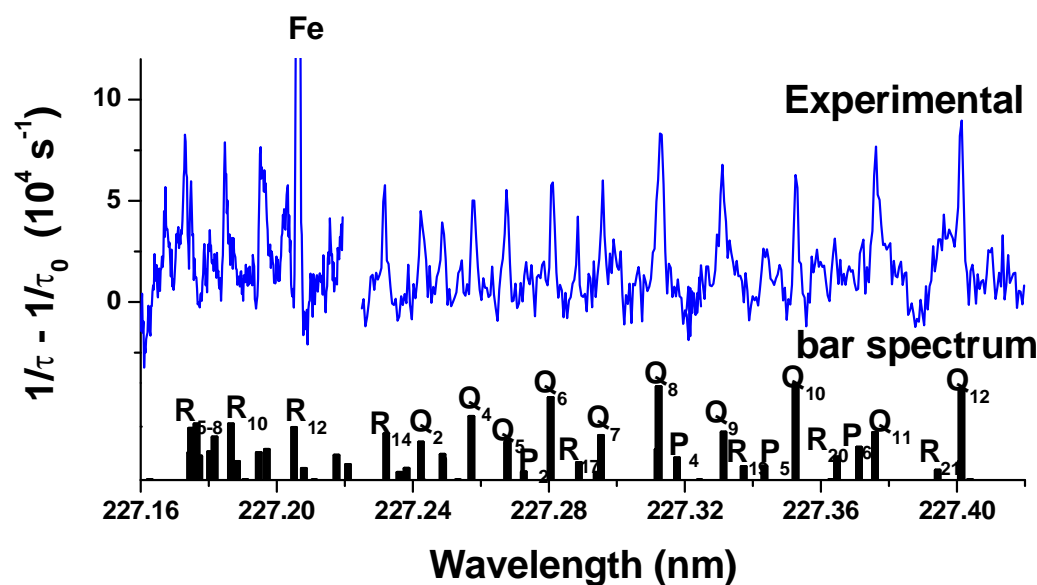
$$\frac{1}{\tau} = \frac{1}{\tau_0} + c \frac{l}{L} \alpha$$

\uparrow
Mirrors lost \uparrow
Lost by absorption

Detection of N₂ (X, v₀=18) by CRDS at 227 nm (a ¹Π_g; v₀=8 → X ¹Σ_g; v₀=18) transition

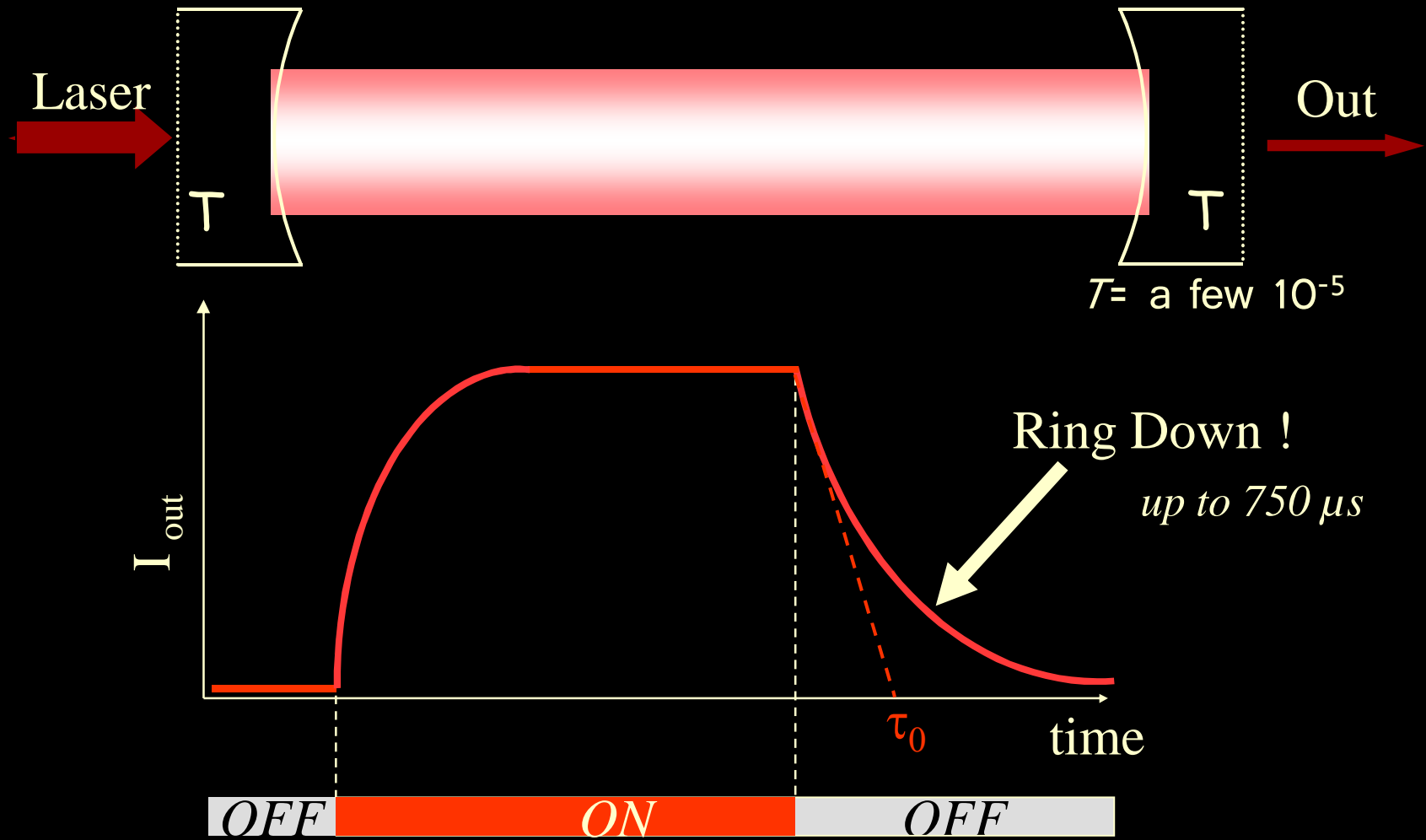


P=2.3 Torr,
I_{discharge}=100 mA

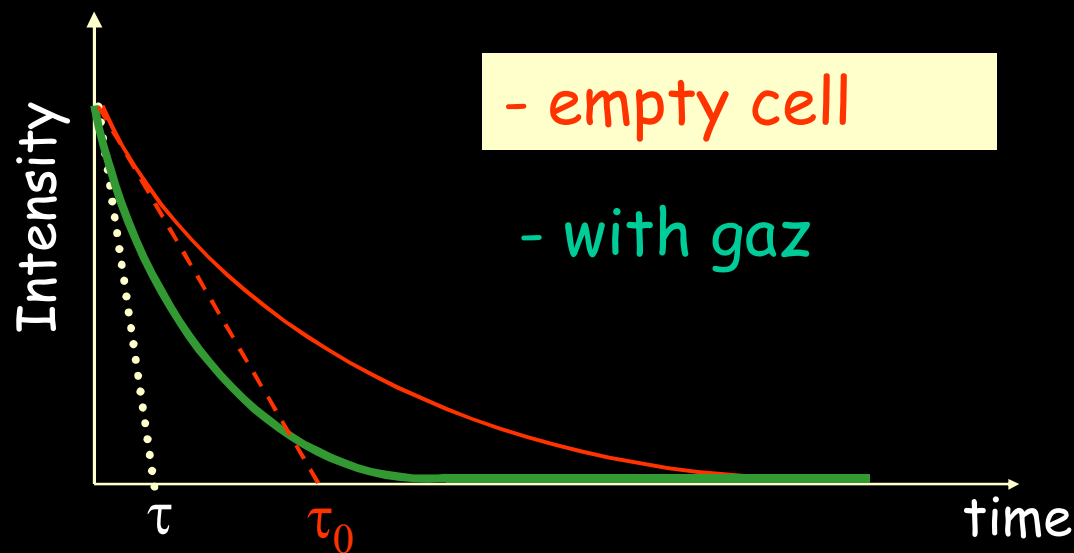
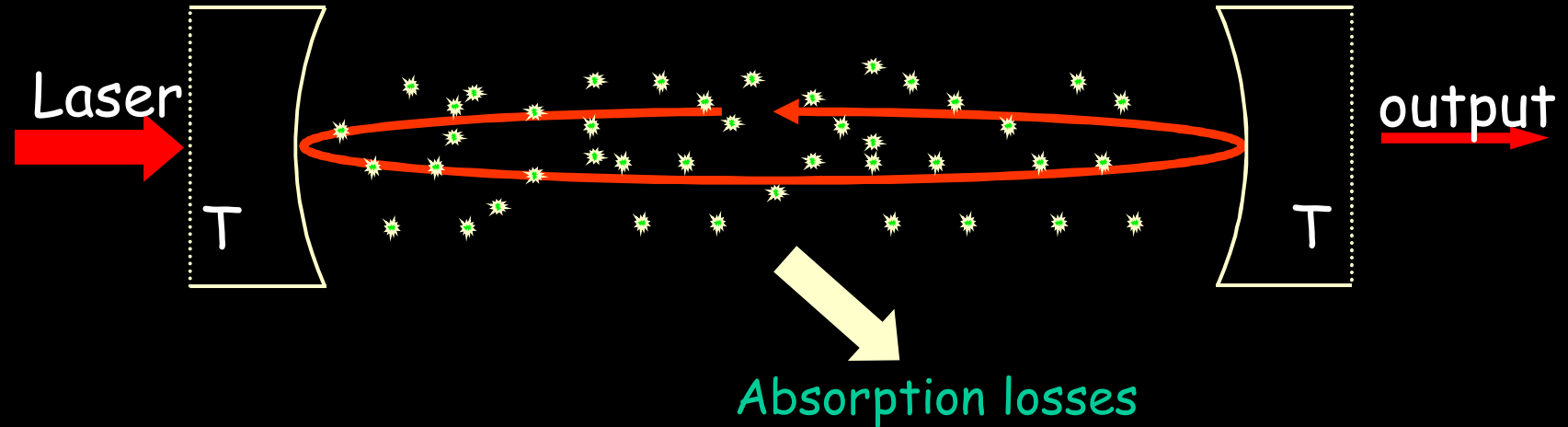


é 0.1% of N₂ molecules
are in v= 18 level

CW-Cavity Ring Down Spectroscopy

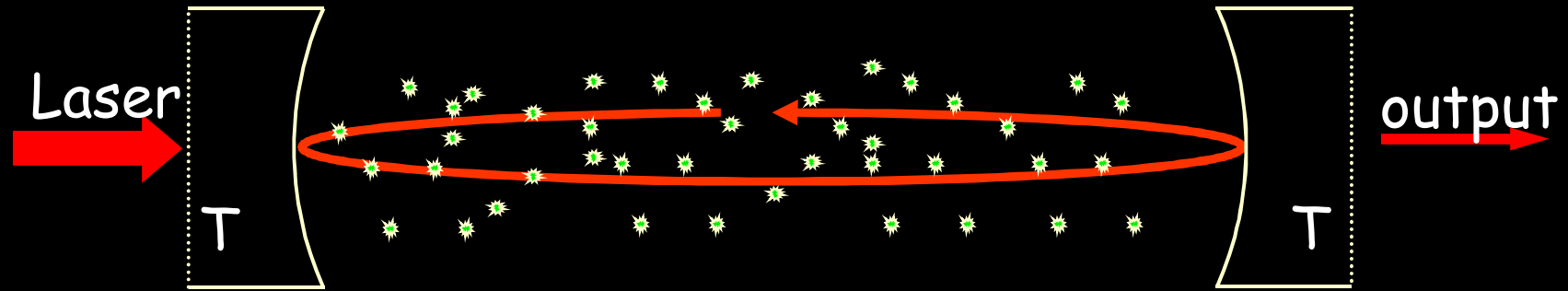


Cavity Ring Down Spectroscopy

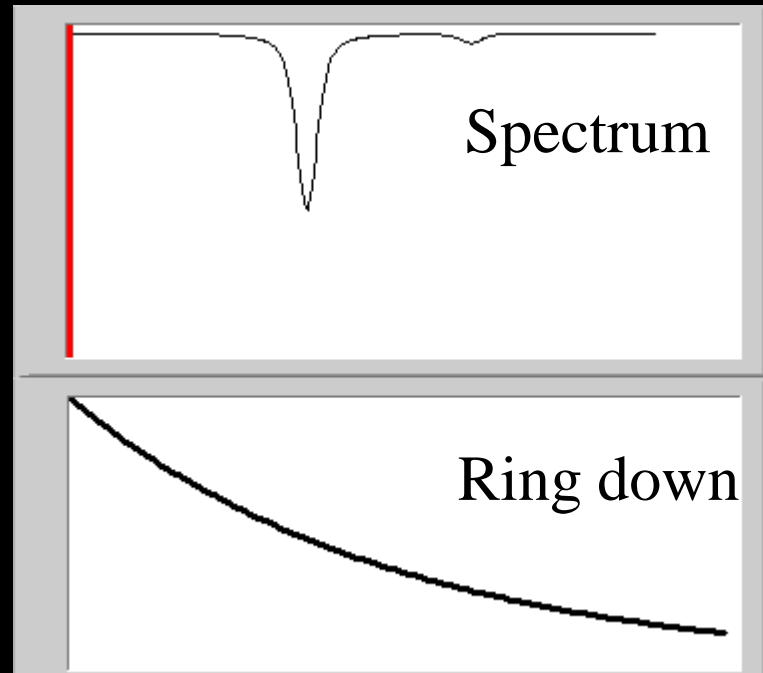


$$\frac{1}{\tau} - \frac{1}{\tau_0} = \alpha c$$

CW-Cavity Ring Down Spectroscopy



$$\frac{1}{\tau} - \frac{1}{\tau_0} = \alpha c$$

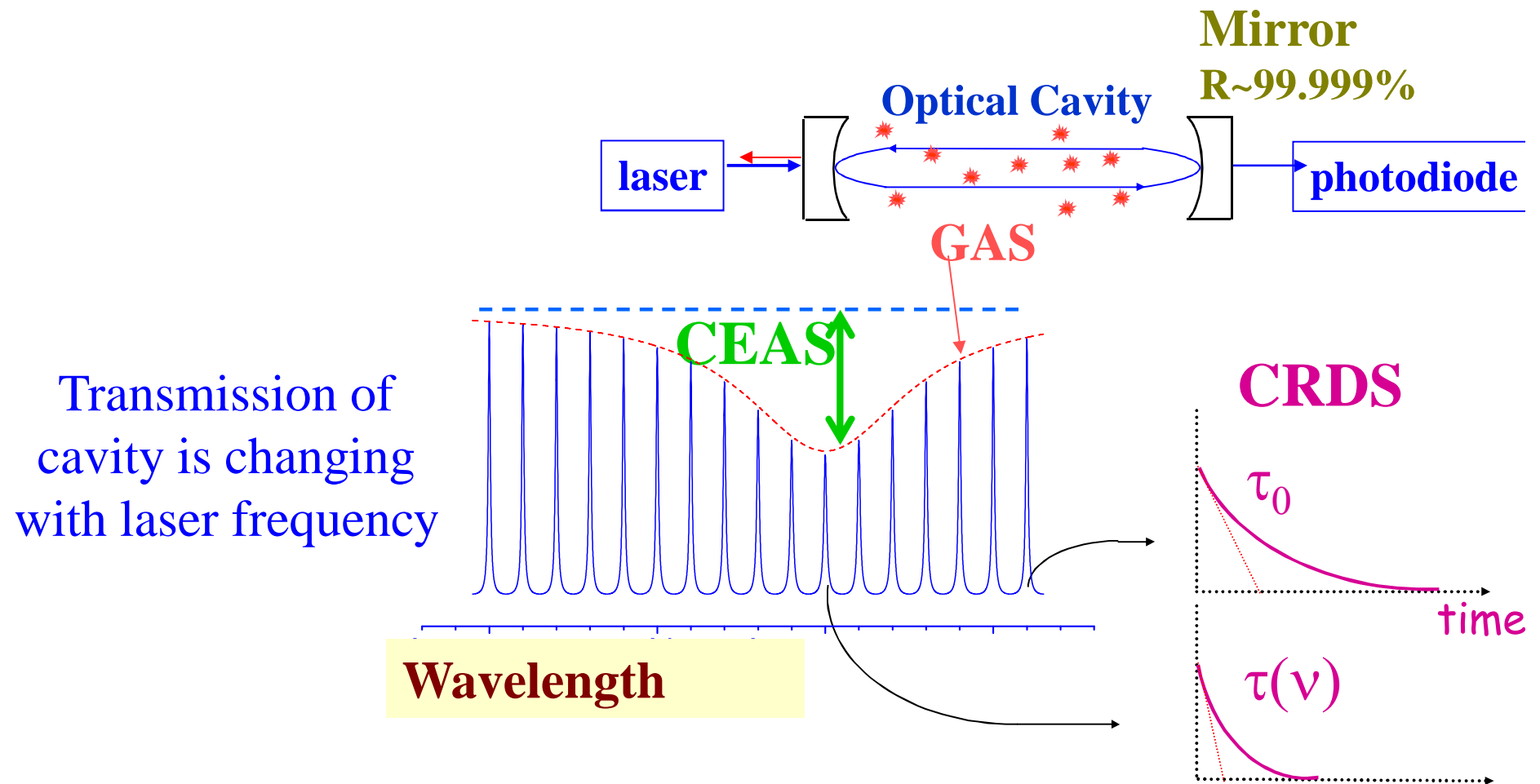


Wavelength scan



variation of the
ring down time

CRDS & Cavity Enhanced Absorption

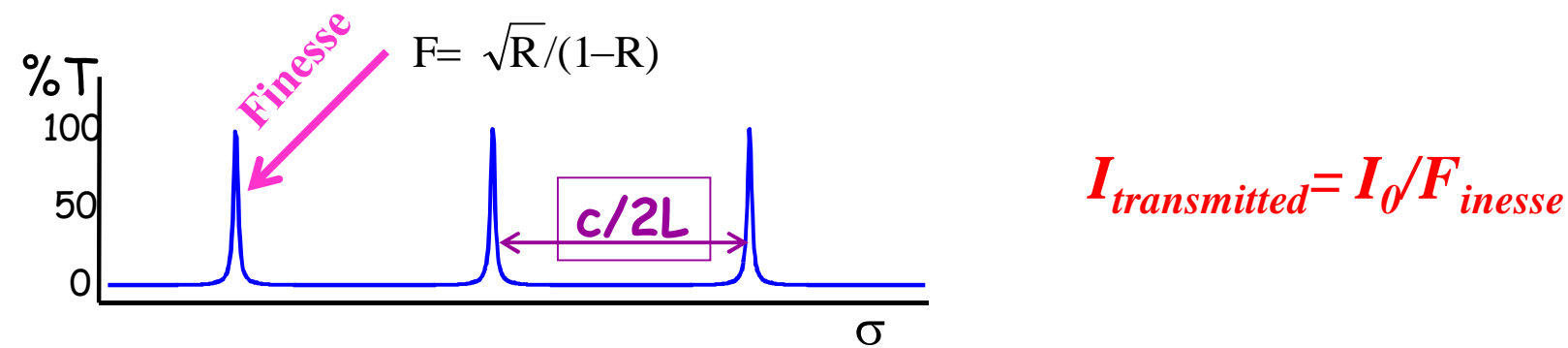


A high sensitivity broad-band mode-locked cavity-enhanced absorption technique with a femtosecond laser

Is it possible to combine broad-band absorption and multipass possibility of the cavity?

If a conventional white source is used

- 1 - With a White cell: only 10-20 passes are possible
- 2- With an optical cavity: Only a small part of the light will be used :



Miraculous solution ?

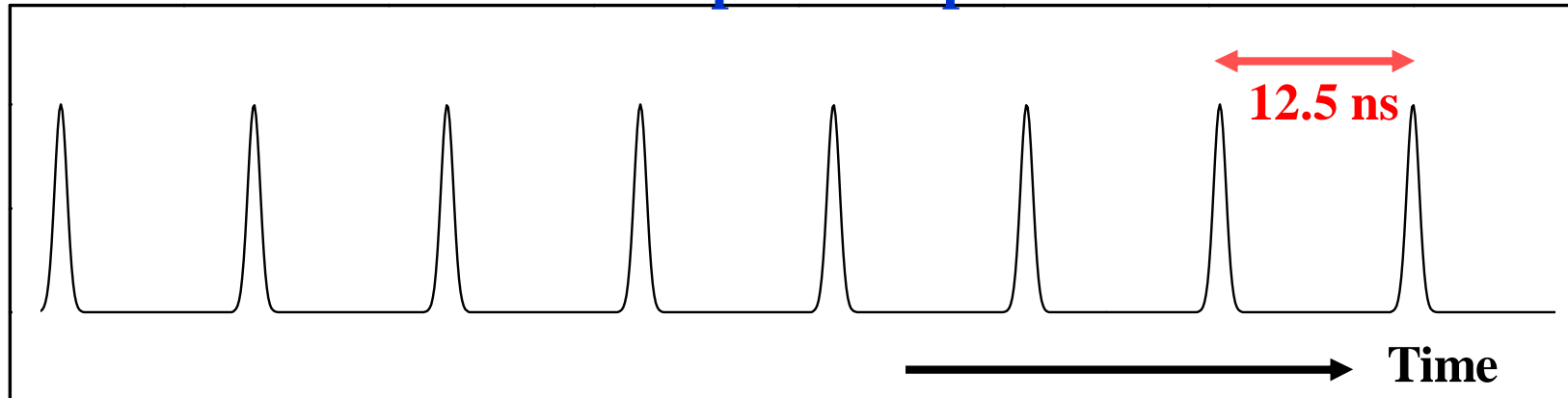
Use a mode-locked femtoseconde laser
for the light source

Why Femtosecond laser source?

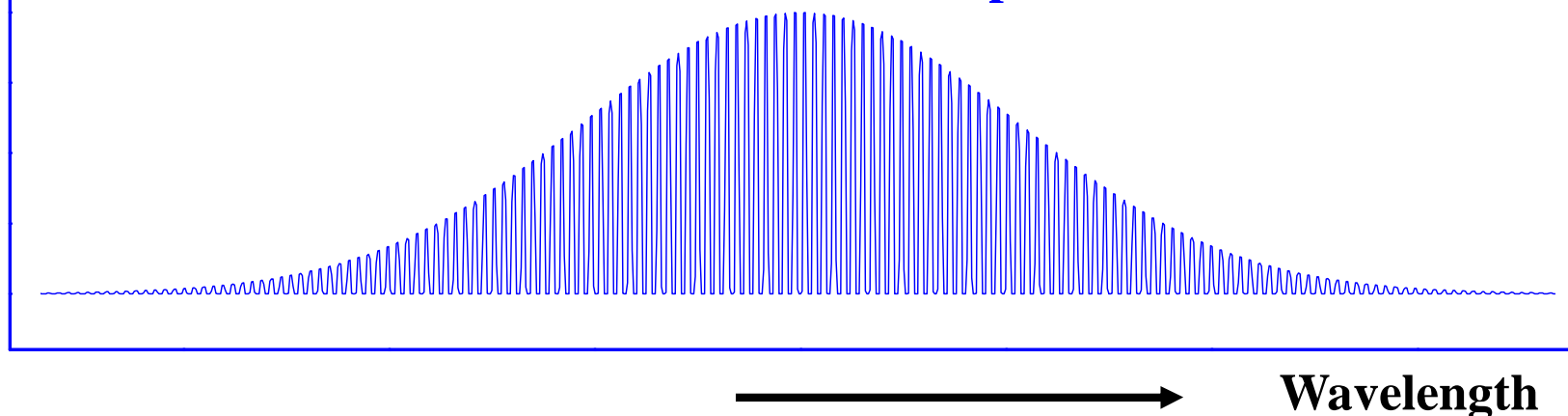
Fourier-transformed smooth and stable laser spectral profile (100 fs \Leftrightarrow 3 nm @ 800 nm) is a good background source for the intracavity sample absorption spectroscopy

Emission spectra of a mode-locked fs laser

Time domain: periodic pulse train

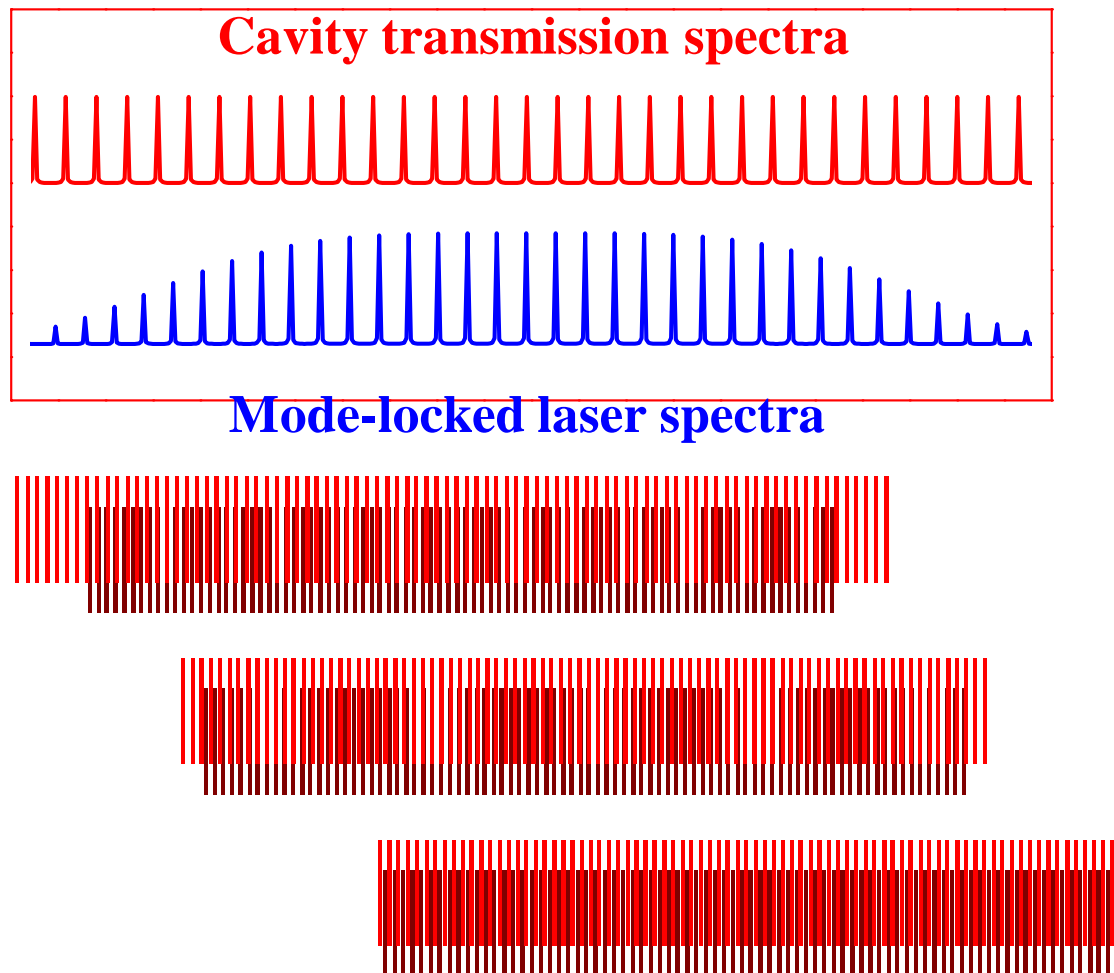


Fourier Transform => Mode-Locked laser spectrum



In a Sa-Ti laser, the spectrum is formed by a comb of $\sim 10^5$ modes, separated by 80 MHz (~ 0.1 pm)

CEAS with mode-locked laser : principle



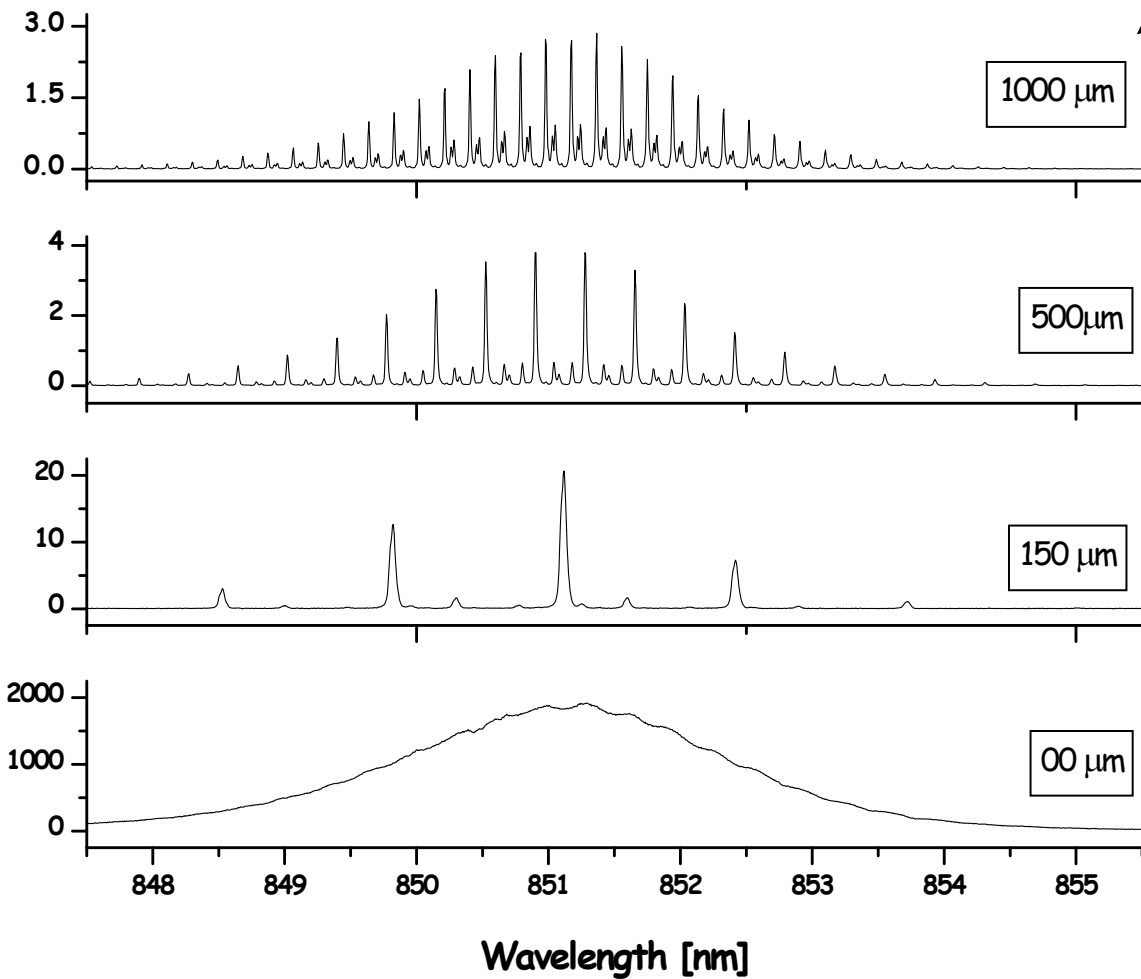
Transmitted spectra= $T_{cav} \times$ Laser spectra

The transmitted spectra by the cavity depends on frequency tuning of these two mode combs :

Tuning the cavity length on can observe beating at different frequenciesí

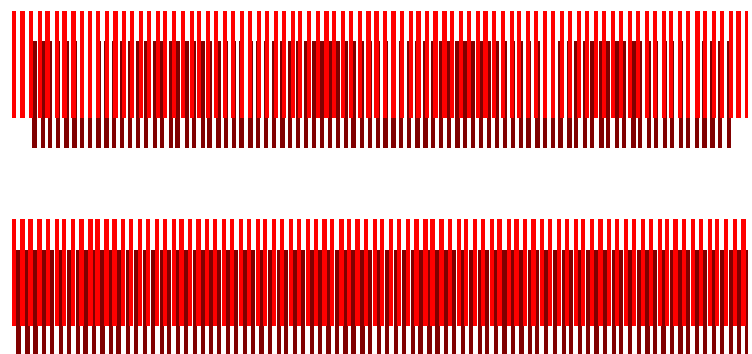
When these two combs are well adjusted, all laser modes build-up and the cavity transmission signal no more beats

Cavity transmission signal

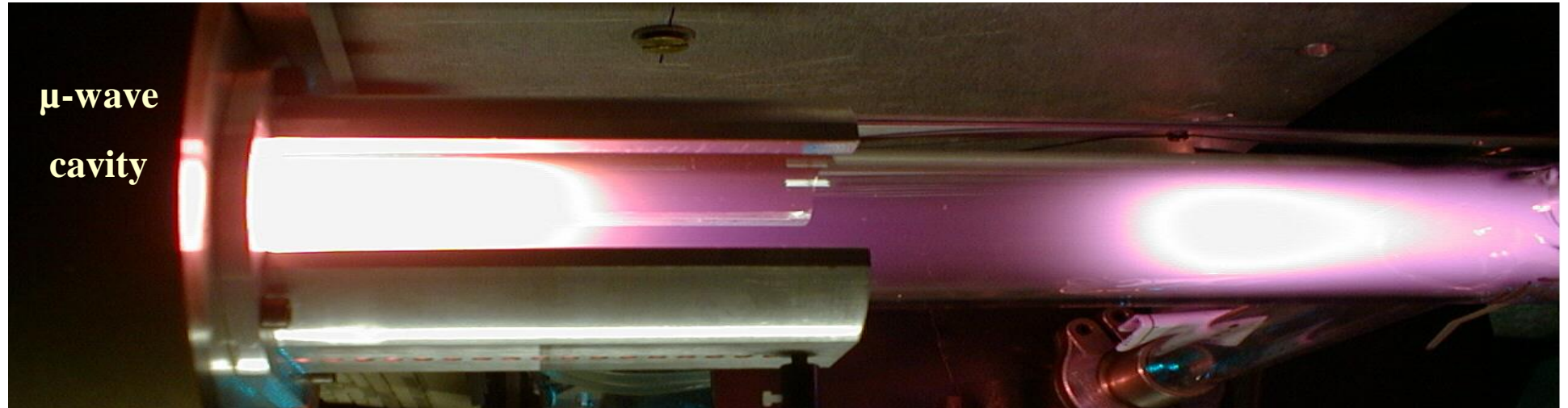


Transmitted Spectra for
different modification of
the cavity length from
magic point, when
 $L_{\text{laser cavity}} = n \cdot L_{\text{F.P. cavity}}$

(minor picks comes
from excitation of
transverse modes)



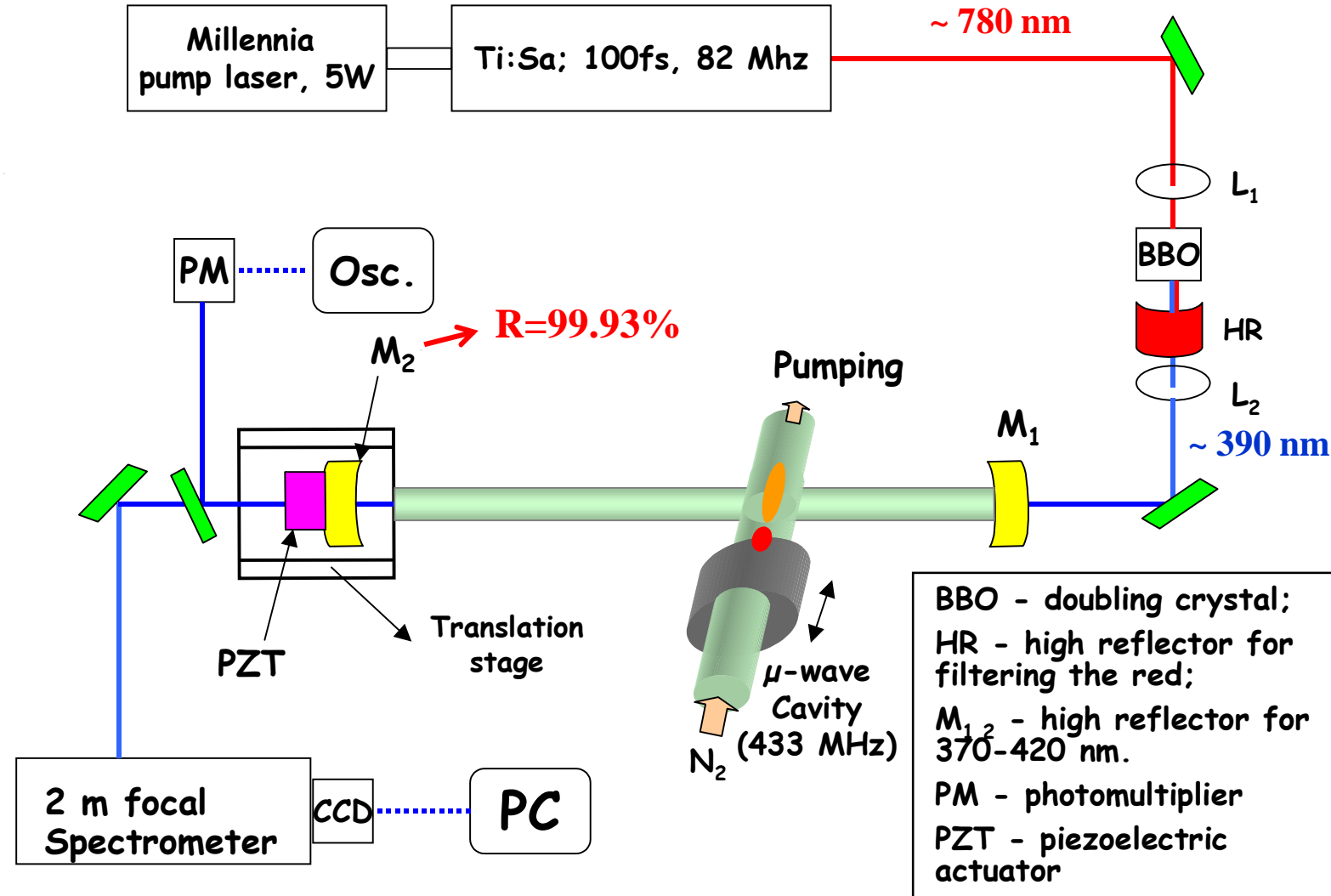
Application of CEBASMF technique for $\text{N}_2^+(\text{X}^2\Sigma_g^+)$ ion density measurement in Short Lived (Pink) Afterglow



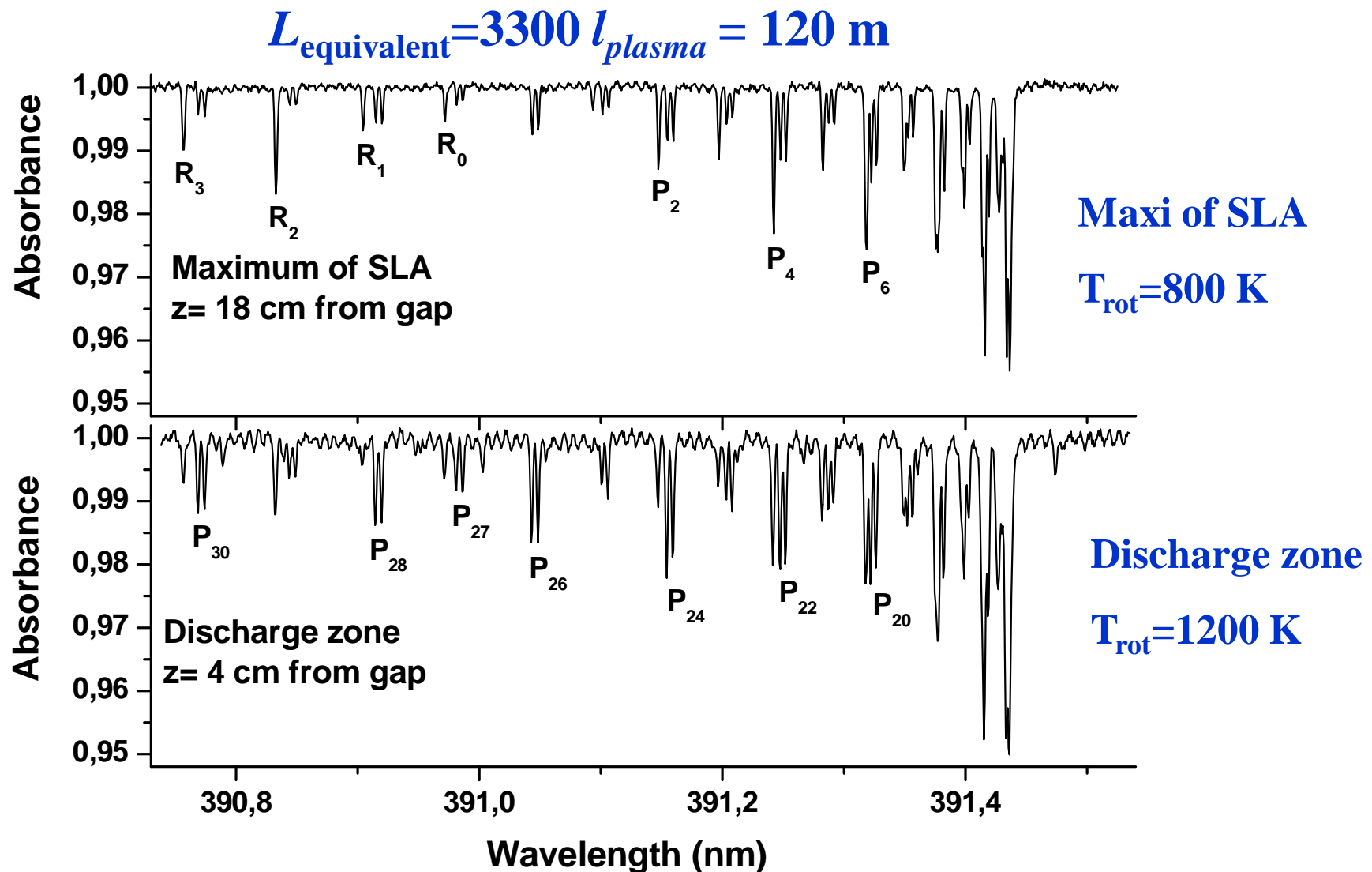
N_2 flow → at about 5 m/s without discharge

$\phi=38$ mm Pyrex tube, $p=440$ Pascal, 300 W @ 433 MHz

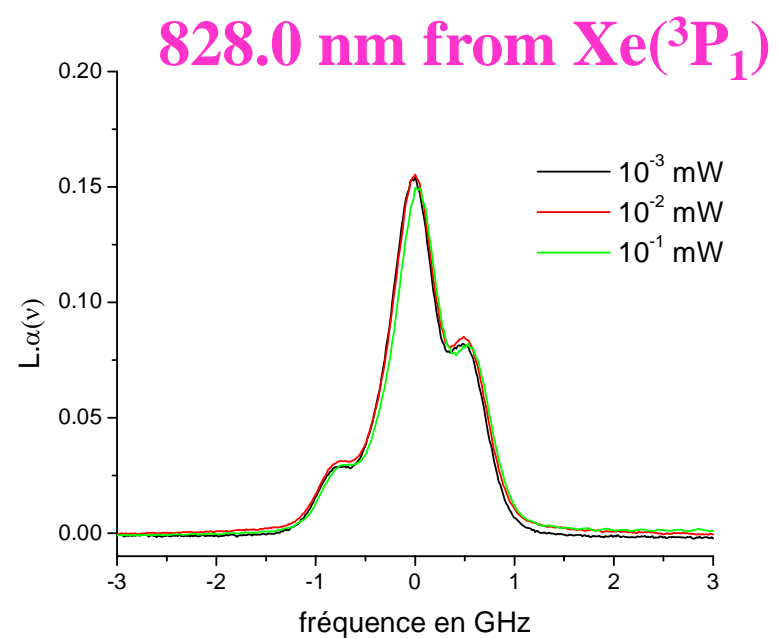
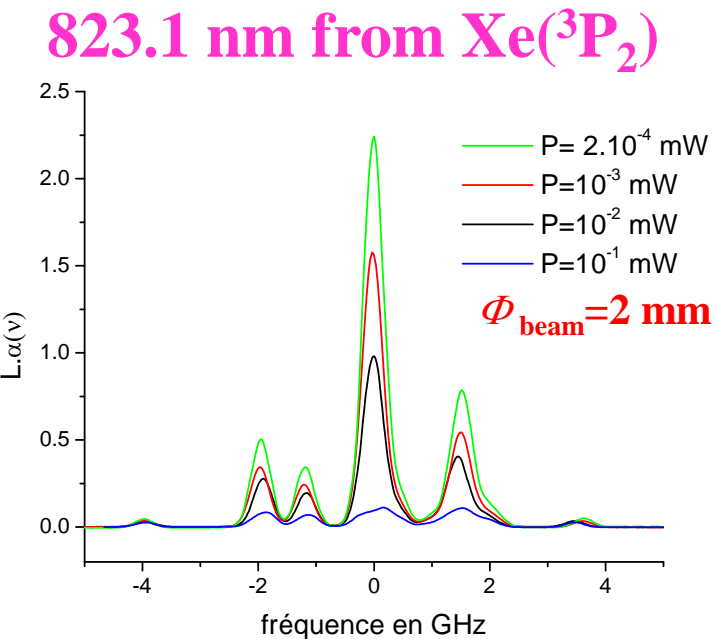
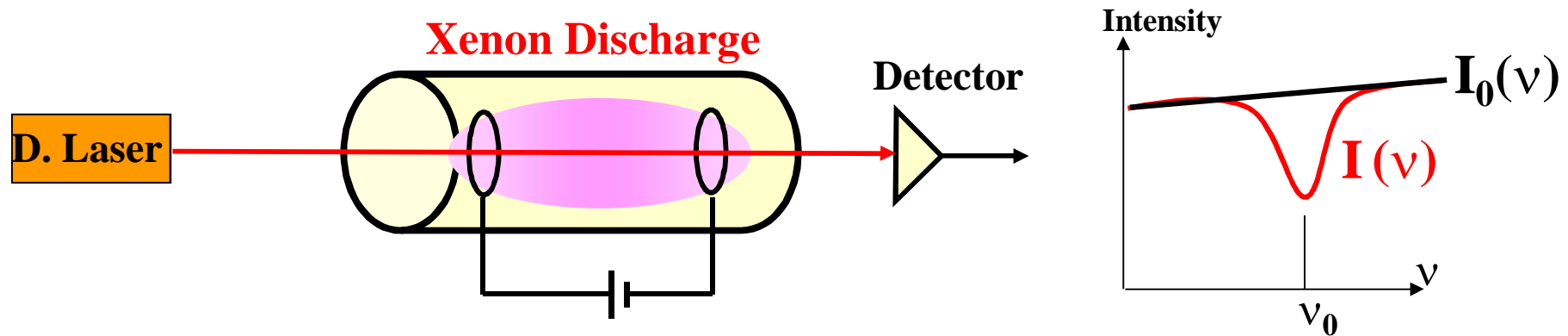
Experimental Setup for CEBA-SMF



**Absorption spectra of $\text{N}_2^+(\text{B} \ ^2\Sigma_{\text{u}}^+; 0 \rightarrow \text{X} \ ^2\Sigma_{\text{g}}^+; 0)$ band
recorded at two positions in Short Lived Afterglow of N_2**



Influence of laser power on line profile and on measured absorption rate



Origin of optical saturation

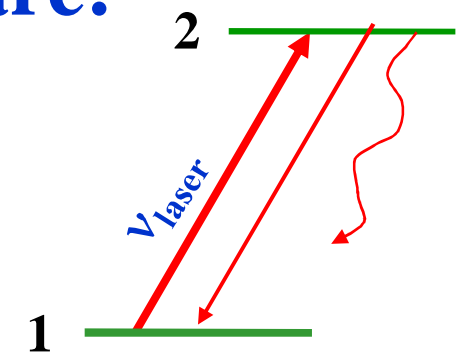
$$\alpha(\nu) = \frac{4hB_{12}}{\lambda\gamma} \left(n_1(\nu) - \frac{g_1}{g_2} n_2(\nu) \right)$$

α becomes no more proportional to n_1

- É 1- Laser beam transfers a significant number of atoms from the lower to the upper state and **n_2 becomes no more negligible compared to n_1 .** (short pulse high power lasers)
- É 2- Atoms in the upper state are lost by radiation, or collisional transfers, to a 3rd state and atoms in the lower state are not renewed fast enough: **the lower state becomes depleted.** (cw lasers)

Rate equations governing the population densities N_1 and N_2 of states $|1\rangle$ and $|2\rangle$ are:

$$dN_1/dt = (B_{21}\rho + A_{21})N_2 - (B_{12}\rho + 1/\tau_1 + \sum_q k_{1,q}M_q)N_1 + C_1$$



$$dN_2/dt = B_{12}\rho N_1 - \left(B_{21}\rho + A_{21} + A_{23} + \sum_q k_{2,q}M_q \right)N_2 + C_2$$

$B_{21} = \frac{g_1}{g_2} B_{12} = \frac{\lambda_0^3}{8h\pi} A_{21}$ is the Einstein coefficient for stimulated emission

we assume $g_1 = g_2$, ρ is the energy density of the beam,

C_i accounts for the repopulation of state $|i\rangle$ from different paths, including diffusion transport into the laser volume and radiative cascades

$$\mathcal{R}_1 = 1/\tau_1 + \sum_q k_{1,q}N_q \quad \text{and} \quad \mathcal{R}_2 = \sum_{i=lower} A_{2i} + \sum_q k_{2,q}N_q$$

are the total relaxation rates of the states

in steady state, ($dN_i/dt=0$) the density difference of states $|1\rangle$ and $|2\rangle$ is:

$$\Delta N = N_1 - gN_2 = \Delta N^0 / (1 + S \frac{\mathcal{R}_2 - A_{21} + g\mathcal{R}_1}{\mathcal{R}_1 + \mathcal{R}_2})$$

Where $\Delta N^0 = N_1^0 - gN_2^0 = \frac{C_1}{\mathcal{R}_1} - \frac{C_2}{\mathcal{R}_2} (g - A_{21}/\mathcal{R}_1)$ is in the absence of laser beam ($\rho=0$),

and

$S = B_{12}\rho/\mathcal{R}^*$ is **The saturation parameter**

related to the **mean relaxation rate** : $\mathcal{R}^* = \mathcal{R}_1\mathcal{R}_2 / (\mathcal{R}_1 + \mathcal{R}_2)$

The resulting population density in the lower state is:

$$N_1 = \frac{C_1(gS + R_2/\mathcal{R}^*) + C_2(gS + A_{21}/\mathcal{R}^*)}{S[R_2 - A_{21} + gR_1] + (R_1 + R_2)}$$

When
 $C_2 \downarrow 0$

$$N_1 = \frac{C_1(gS + R_2/\mathcal{R}^*)}{S[R_2 - A_{21} + gR_1] + (R_1 + R_2)}$$

Larger S is, lower the measured population will be

When $\rho \rightarrow 0$, $N_1 = \frac{C_1}{\mathcal{R}_1}$

For $\rho \rightarrow \infty$ $N_1 = \frac{g(C_1 + C_2)}{\mathcal{R}_2 - A_{21} + g\mathcal{R}_2}$

Spectral line profiles

Homogeneous linewidth: For a given transition it is identical for all atoms:

Its shape is a Lorentzian

$$\phi_L(\nu-\nu_0) = \frac{1}{2\pi} \frac{\delta\nu_L}{(\nu-\nu_0)^2 + (\delta\nu_L/2)^2}$$

Natural linewidth:

$$\delta\nu_n(FWHM) = \frac{1}{2\pi\tau}$$

Power broadening: $\delta\nu_S = \delta\nu_n \sqrt{1 + S_0}$ S₀ at the line center ν₀

Inhomogeneous linewidth: results from collective effects, for example thermal motion of atoms (**Doppler broadening**):

Its shape is a Gaussian

$$\phi_D(\nu-\nu_0) = \frac{2\sqrt{\ln(2)/\pi}}{\delta\nu_D} \exp -4\ln(2) \frac{(\nu-\nu_0)^2}{(\delta\nu_D)^2}$$

Doppler linewidth: $\delta\nu_D(GHz) = (2\nu_0/c)\sqrt{2\ln 2(RT/M)} = 7.16 \cdot 10^{-16} \nu_0 \sqrt{T/M}$

For sodium 589.1 nm line ($\tau=16$ ns) at 500 K:

$$\delta\nu_n = 0.01 \text{ GHz}$$

$$\delta\nu_D = 1.7 \text{ GHz}$$

Estimation of saturation parameter S

For a cw laser:

$\lambda = 590 \text{ nm}$;

$\tau_2 = 16 \text{ ns}$; hence $R_2 = 1/\tau_2 = 6.25 \cdot 10^7 \text{ s}^{-1}$

But $A_{21} = 6 \cdot 10^6 \text{ s}^{-1}$;

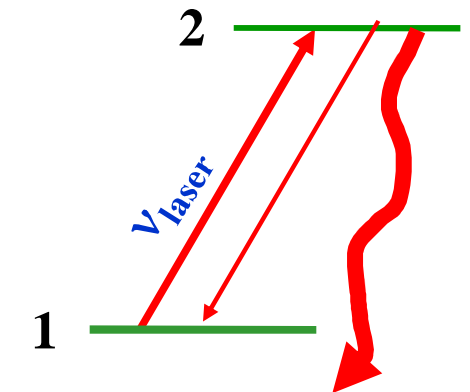
$R_1 = (1/\text{transit time inside a beam of } \phi=2 \text{ mm}) = (0.5 \text{ km.s}^{-1})/(2 \text{ mm}) = 2.5 \cdot 10^5 \text{ s}^{-1}$

Laser power: $P = 1 \text{ mW}$; $\Delta\nu_L = 1 \text{ MHz} \ll 1/(2\pi\tau_2)$;

Laser beam diameter = 2 mm

We can calculate

$$S = \frac{B_{12} * \rho}{R_1} = 20$$



Hence the density measured by absorption will not be correct with so large S value

because $N_1 = N_1^0 / (1 + S)$ However,

as $\delta\nu_S = \delta\nu * \sqrt{1 + S} = 4.5 * \delta\nu = 45 \text{ MHz}$ is much smaller than the Doppler width (1.7 GHz), the line profile can still provide the gas temperature

A photograph of a vast, turbulent sky filled with rolling clouds. The lighting is low, creating deep shadows and bright highlights that suggest either a setting sun or a rising moon. The clouds are thick and layered, creating a sense of depth and atmosphere. In the bottom right corner, the word "Merci" is written in a large, white, sans-serif font.

Merci